

MATERIALS AND METHODS

Materials

1. Reactor–The acrylic clear reactor has 9 cm. in diameter and 150 cm in height. Polypropylene beads with a diameter of 3, 6, and 10 mm. are used as the floating media in downflow flocculator.
2. Raw water tank 1000 L
3. Submerge pump capacity 100 L/min, Ogarmar
4. Constant head tank
5. Rapid mixing device
6. Peristaltic pump master flex for feeding chemical, Masterflex, Model MP3, Evela
7. Piezometer
8. Flow meter: MMA Series caution, 690 kPa, 100 PSIG Max., 54°C, 130°F Max.
9. Coagulant : Polyaluminium chloride (PACl)
10. Kaolin clay 200 mesh
11. Turbidity meter, Model 2100 P, Hach
12. pH meter, Model 215, Denver Instrument
13. Glass ware for Analysis
14. Sieve sand
15. Microscope : CHS/CHT, Olympus, Model CHS, 220/240 V ~50-60 Hz, 0.15/0.14 A, Lamp 6 V, 20 w, same type fuse only 0.63 A
16. Glass microscope slide
17. Digital camera : Finepix S5000, FUJI, 2120 x 2816 pixels, camera lens was macro lens with ISO 200, bracketing $\pm 1/3$ EV, F-6.3, shutter exposure of 1/800 sec and flash ± 0
18. Light-source, 5 watt
19. Image processing program : Matlab version 7, Sonic CinePlayer

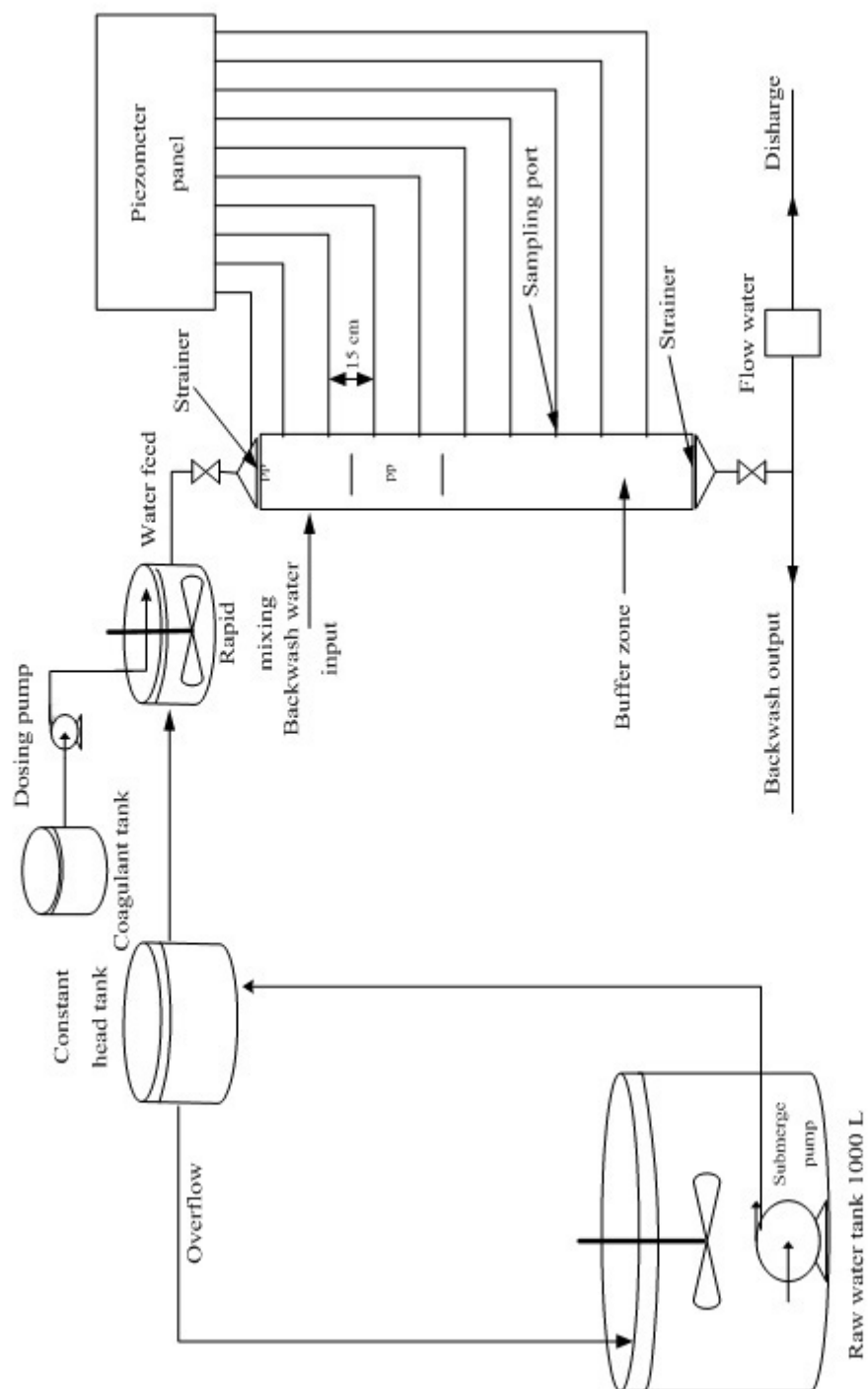


Figure 4 Schematic of a floating-media-flocculation system set-up for operating



Figure 5 Experimental setup as bench-scale at Kasetsart University



Figure 6 Floating plastic media flocculator column with 3-mm and 10-mm media sizes

Methods

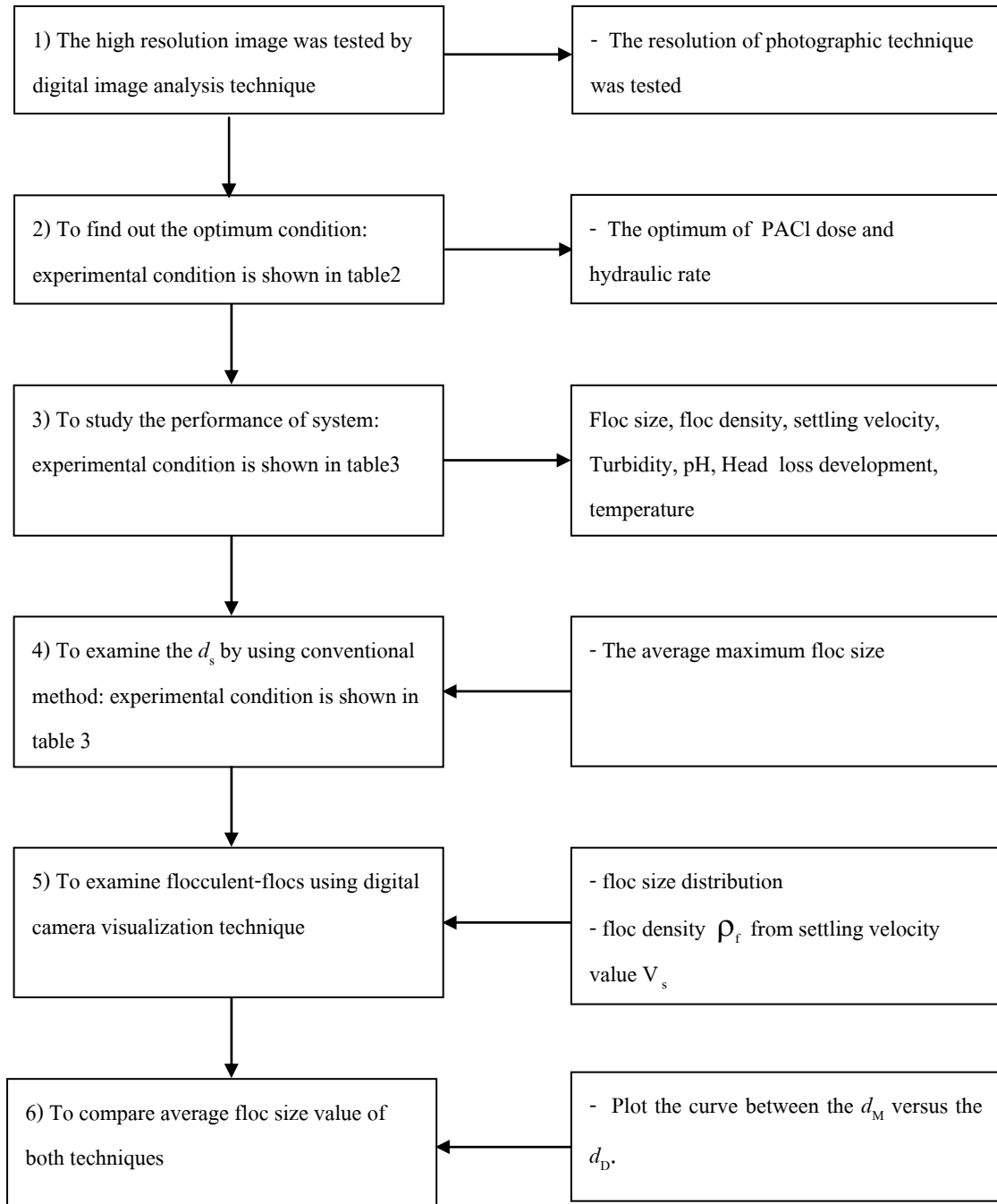


Figure 7 Experimental methodology

1. The high resolution image is tested of using photographic techniques

1.1 The resolution from the photographic techniques in taking photographs and video pictures were tested of high resolution images. A high resolution digital camera (FUJI FinePix S5000) was used to record the images. The camera has a sensor matrix consisting of 2120 (horizontal) x 2816 (vertical) pixels. Each pixel records using 24-bits, there are 256 gray scale levels for each image pixel in size. The camera lens was macro lens with ISO 200, bracketing $\pm 1/3$ EV, F-6.3, shutter exposure of 1/800 sec and flash ± 0 were found to provide good results for images. The flocculent-floc could observe by focusing on a plane distance 4.5 cm (haft of diameter of column) behind the wall of the column.

1.2 The video picture real-time capturing was 320 x 245 pixels. The time measuring resolution of digital video is 10 second.

1.3 The most suitable positions of a digital camera and light sources were tested. The position of a digital camera was in front of the column at the buffer zone next to the end of the media-layer. The components of the image analysis system are illustrated in Figure 6.

1.4 Sand sieve : using a splitter, obtain about 100 grams of sand, only 5 screens (72 μm , 150 μm , 300 μm , 600 μm , and 1000 μm) and sieve for 15 minutes. The sand was released from the top of the column, and while passing through the observation region in the acrylic-column, image and video were obtained using a digital camera for each size, respectively. Sand sieving was used to confirm number and size counting.

1.5 The image processing programs were tested with the flocculent-imaged and video that was recorded. The image processing programs were tested with images and video that was recorded. The image processing programs were tested for accurate ability to count number and flocs size. MatLab Version 7 program examined floc size distribution that was used to measure the number and size of floc. The image processing steps are as follows:

Step one: The file format had to be converted from JPEG file to TIFF file. For tiled TIFF images, it can read only the tiles that encompass the region specified by rows and columns, improving memory efficiency and performance which other file format can

not read encompass the region. Rows and columns must be either two or three element vectors.

Step two: The color images were converted to gray scale images.

Step three: The images were cropped, retaining only the centre of each, one from three image size (vertical) and one from five (horizontal) because the column is round. Therefore, left and right parts of images might not get accurate images.

Step four: Ranges of gray scale index were selected to separate flocculent-flocs from background. Many image contain a significant amount of background gray level variability. Thus, a gray level threshold which is appropriate to detect a given at center may not be appropriate at an edge.

Step five: The intensity image was converted to binary because the MatLab program can count numbers of objects in black (0) and white (1) only. In this step the background is white and flocculent-flocs are black.

Step six: The conversion the white background to a black background and black flocculent-flocs to white flocculent-flocs.

Step seven: Number and flocs size were counted. The program, written in Matlab version 7, was integrated into a Microsoft Excel spreadsheet, allowing both tabular and graphic output. In the last step flocs distribution graph was plotted between number and size of flocs versus operating time.

2. Optimum condition of floating plastic media flocculator (Run no.1-13)

2.1 Synthetic raw water was created by adding kaolin clay to tap water at turbidity level of 80 NTU to be used in the experiment.

2.2 Raw water was pumped into constant head tank continuously, synthetic raw water into the rapid mixing device.

2.3. The feed line ahead of rapid mixing device (approximately one-second mixed). Polyaluminium chloride was fed in using a chemical dosing pump. Subsequently, coagulated water was continuously supplied into the column.

2.4 The experimental system was operated over a short term run following the conditions that are shown in Table 4.

2.5 The water from outlet sampling port was sampled and analyzed every 30 minutes in the first 3 hours and every 1 hour in the next 3 hours, respectively. The experimental parameters were composed of turbidity, pH, floc size, temperature.

2.6 The head loss development and expanded depth were recorded every 30 minutes during the first 3 hours and every 1 hour during subsequent 3 hours.

3. Performance of floating plastic media flocculator (Run no.14-27)

3.1 The floating media was changed following the conditions shown in Table 5.

3.2 The optimum condition was used to operate system. The experiment was done by repeating the experiment no. 2.1 to 2.6.

4. The maximum flocs size (d_M) were observed using microscopic analysis

4.1 The resolution of microscopic technique observation flocculent-flocs was examine. The resolution of microscopic technique was observed flocculent-flocs.

4.2 The average maximum flocs size (d_M) was observed using classical technique.

5. Flocculent-flocs were examined using digital image analysis

5.1 Flocs size distribution was examined by digital photographs.

5.2 The video pictures for calculated settling velocity (V_s) from the settling velocity occurred (w) minus the hydraulic rate (v). Then the settling velocity value was obtained to calculate the density of floc (ρ_s) Stokes' equation.

$$V_s = w - v \quad (1)$$

Where:

V_s = the settling velocity

w = the settling velocity occurred

v = the hydraulic rate

$$V_s^2 = \frac{4g}{3C_D} \left(\frac{\rho_s - \rho}{\rho} \right) d \quad (2)$$

Where:

V_s = the Settling Velocity

ρ_s = mass density of floc

ρ = mass density of liquid

g = acceleration due to gravity

d = floc size

6. Flocculent-flocs size was compared by using both techniques

The comparison between the floc size measure by a microscope analysis (d_M) and floc size analyzed by digital image analysis (d_D) was carried out.

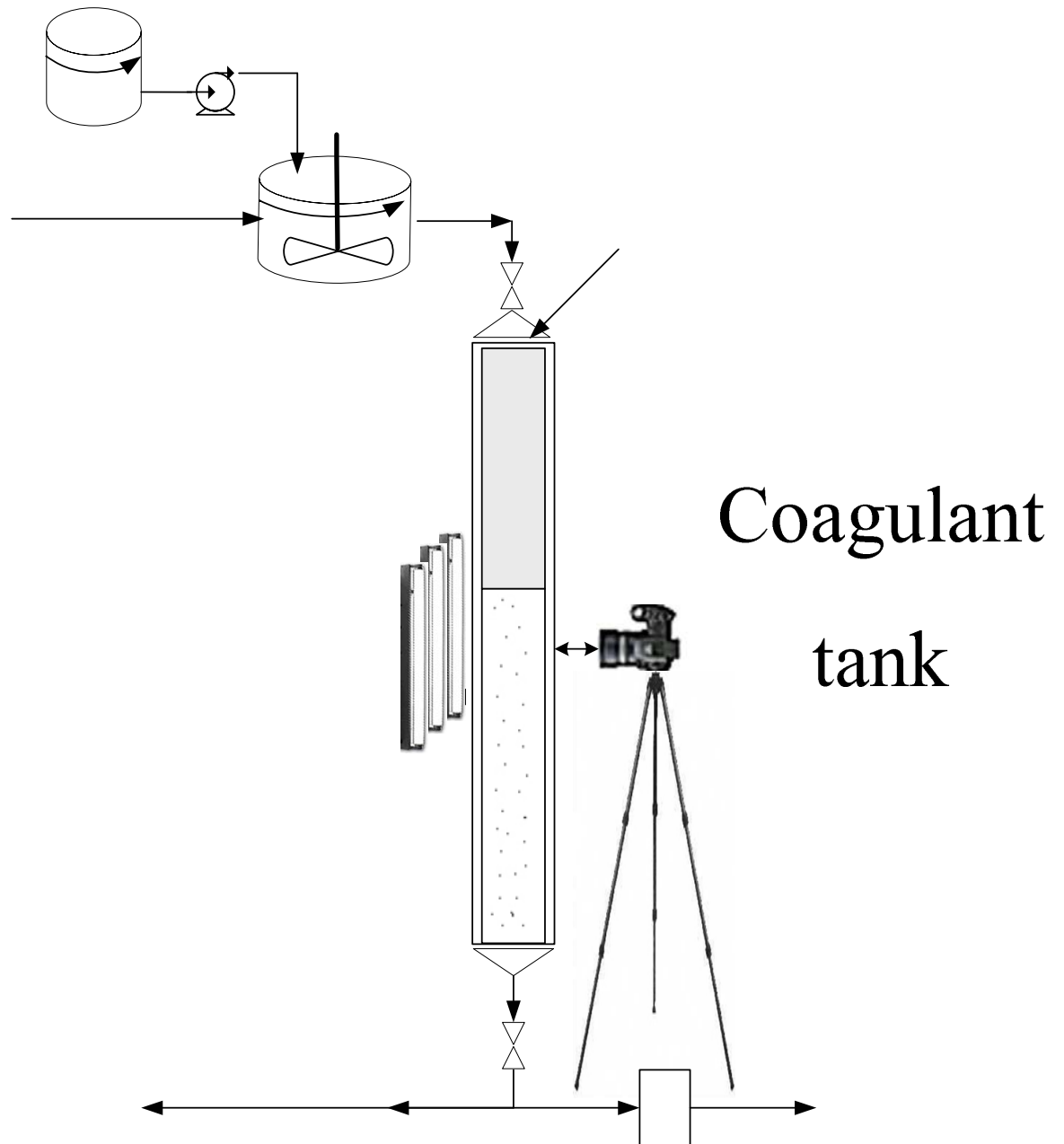


Figure 8 Schematic of the experimental system set-up for recording floc images.

Table 4 Experiment schedule of the optimum condition

Run No.	Media Size (mm)	Hydraulic Rate $\text{m}^3/\text{m}^2\text{-h}$	Flocculent Dose (mg/L)	Media Depth (cm)	Analytical Parameters
1 (Single Media)	3	2.5	2.5	60	Turbidity, pH floc size,
2 (Single Media)	3	2.5	5.0	60	
3 (Single Media)	3	2.5	10.0	60	
4 (Single Media)	3	5.0	1.3	60	Number of floc,
5 (Single Media)	3	5.0	2.5	60	floc density,
6 (Single Media)	3	5.0	5.0	60	settling velocity,
7 (Single Media)	3	5.0	10.0	60	Temperature,
8 (Single Media)	3	5.0	40.0	60	expanded depth &
9 (Single Media)	3	10.0	1.3	60	head loss development
10 (Single Media)	3	10.0	2.5	60	
11 (Single Media)	3	10.0	5.0	60	
12 (Single Media)	3	10.0	10.0	60	
13 (Single Media)	3	10.0	40.0	60	

Table 5 Experiment schedule of the performance of floating-media flocculator

Run No.	Media Size (mm)	Hydraulic Rate $\text{m}^3/\text{m}^2\cdot\text{h}$	Flocculent Dose (mg/L)	Media Depth (cm)	Analytical Parameters
14 (Single Media)	3	2.5	2.5	30	
15 (Single Media)	3	2.5	2.5	60	Turbidity, pH
16 (Single Media)	6	2.5	2.5	30	floc size,
17 (Single Media)	6	2.5	2.5	60	Number of floc,
18 (Single Media)	10	2.5	2.5	30	floc density,
19 (Single Media)	10	2.5	2.5	60	settling velocity,
20 (Single Media)	3.6	2.5	2.5	30	Temperature,
21 (Single Media)	3.6	2.5	2.5	60	expanded depth &
22 (Single Media)	3.10	2.5	2.5	30	head loss development
23 (Single Media)	3.10	2.5	2.5	60	
24 (Single Media)	6.10	2.5	2.5	30	
25 (Single Media)	6.10	2.5	2.5	60	
26 (Single Media)	3,6,10	2.5	2.5	30	
27 (Single Media)	3,6,11	2.5	2.5	60	

RESULTS AND DISCUSSION

1. The high resolution image was tested using photographic techniques

This aim study determined the most high resolution images from position of a digital camera, light-sources and performance image processing programs. The most suitable position of a digital camera was in front of the column at the buffer zone next to the end of the media-layer. The digital camera must be this position because photographs are needed of real flocculent-floc size when the flocculent-flocs started to leave the media layer. If the position is below, flocculent-floc might contact between the other flocs to form larger floc. The most suitable positions of light-sources, Figures 9(a) and 9(b) shown the positions of light-sources. Figure 9(a), the position light-sources were the left and the right sides of the column. An image was not clear and sharp for observation flocculent-flocs. At the same resolution photography, Figure 9(b) the illuminated by 3 light-sources were on the opposite side of the column from the digital camera to provide back-lighting, which produce flocs image as shadows.

The flocs images were analyzed with image processing program MatLab version 7. The floc video that was recorded was analyzed with the Sonic CinePlayer. MatLab version 7 is a high-performance language for technical computing. It integrates computation, visualization, and programming in an easy-to-use environment where problems and solutions are expressed in familiar mathematical notation. This program has been widely used in recent research and engineering applications.

There are other sources of noise in a digital image besides noise contamination of the pixel brightness. The act of sampling, cutting up the image into row and column, is also an important source of noise which is of particular significance when the goal is image analysis. The potential effect of this kind of noise can be illustrated with the relatively simple problem of measuring the area of a two dimensional object that the best the measure of the area of an analog object given its digital representation is to simply count the pixels associated with the object. The use of the term of the best estimate means that the estimate is unbiased and that the variance goes to zero

(precise) as the sampling density increase. We assume here that the pixels belonging to the object have been labeled thus producing a binary representation of the object.

Imaged was examined in Photoshop program 1 pixel equal to $35.5\text{ }\mu\text{m}$ multiply 1.4-fold of image that is $56\text{ }\mu\text{m}$. Because resolution image consisting of 2120×2816 pixels that numerous in pixel. An image is too large to be contained within its display; it creates a compressed view with a roaming window, and a full resolution view. The roaming window is moved around on the compressed view, to select part of the large image for high resolution display. The advantage of large image format is that we analyze data from the high resolution view. This gives the best possible accuracy. At the same time, we can position ourselves very easily using the compressed view. Because large images are handle so well. If the images are not clear and sharp contrasted from the background, there is a possibility of over-sizing due to fuzziness at the edges of the flocculent-floc. Flocculent-floc below $56\text{ }\mu\text{m}$ could not be reliably measured using their camera system in photographs. Video pictures were low resolution (320×245 pixels) flocculent-floc size should not be below $150\text{ }\mu\text{m}$ which could not measure flocculent-floc every sizes.

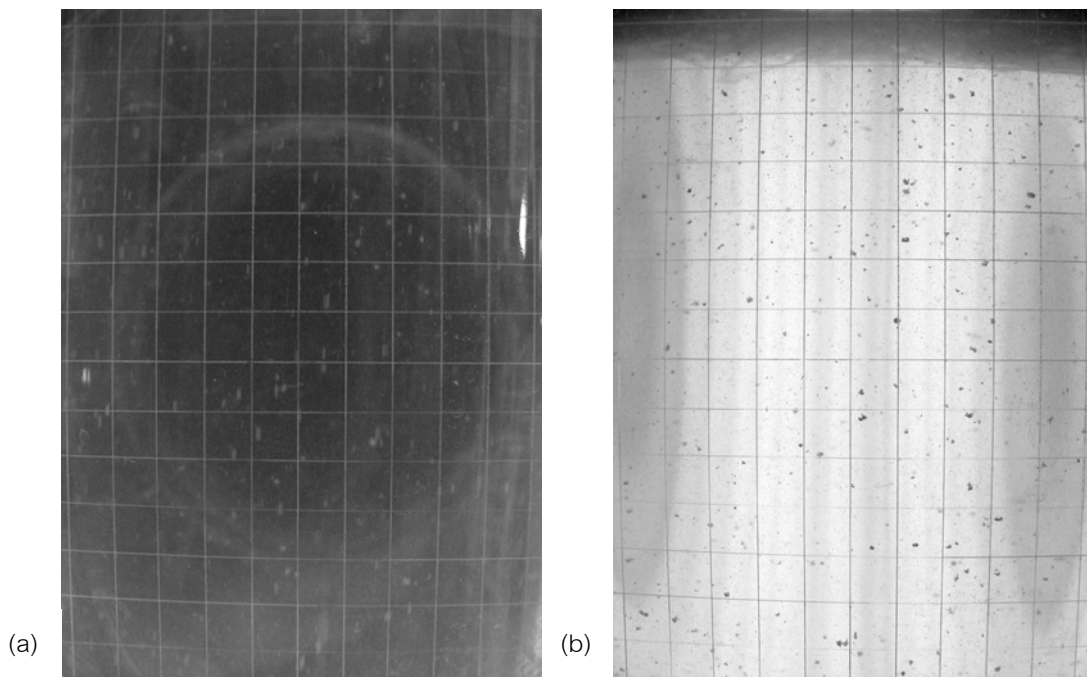


Figure 9 The positions of illuminates (a) the illuminates was side of the digital camera, (b) the illuminates was opposite side of the column.

2. Optimum condition of floating-plastic media flocculator

This aim study of determine the optimum flocculent dose and hydraulic rate in operation in a flocculator. The polypropylene beads 3 mm in diameter and a layer depth of 60 cm was used during operation. The synthetic raw water was prepared by dissolving kaolin clay in tap water to produce a sample with turbidity of 80 NTU, approximately. The performance of floating media flocculator was examined using different doses of polyaluminum chloride (PACl). For flocculent, a stock solution of PACl was prepared by dissolving PACl in deionized water to a concentration of 12.5% (1.25 mg/L), 25% (2.5 mg/L), 50% (5 mg/L), 100 % (10 mg/L) and 400% (40 mg/L). The system was operated using different hydraulic rates of 2.5, 5 and 10 m³/m²-h.

2.1 Effect of polyaluminium chloride dosage

2.1.1 Effect of PACl doses on turbidity removal

The system performance in terms of turbidity removal at different PACl doses and the hydraulic rate of 2.5 m³/m²-h. From the results, the turbidity removal at PACl doses of 2.5 mg/L and 5 mg/L were not significantly different and rather constant at a high value of 96.4% in the long-term operation as shown in figure 10.

The effects of different PACl doses at the hydraulic rates of 5 m³/m²-h and 10 m³/m²-h on turbidity removal, respectively, as shown in Figure 11 and Figure 12. In Figure 11, the high turbidity removal, which was more than 85%, at PACl doses of 40 mg/L, 10 mg/L, 5 mg/L, 2.5 mg/L and 1.25 mg/L deteriorated after 60, 90, 150, 240 and 600 minutes of operating time, respectively. It indicated that the higher PACl performed faster breakthrough of turbidity. And Figure 12 also shows the same results. The quality of effluent water deteriorated over 30, 60, 60, 90 and 150 minutes of operating time at PACl doses of 40 mg/L, 10 mg/L, 5 mg/L, 2.5 mg/L and 1.25 mg/L, respectively. Figures 11-12, it was observed that application of PACl dose of 2.5 mg/L produces a good effluent in terms of low turbidity (high turbidity removal) for any hydraulic rate.

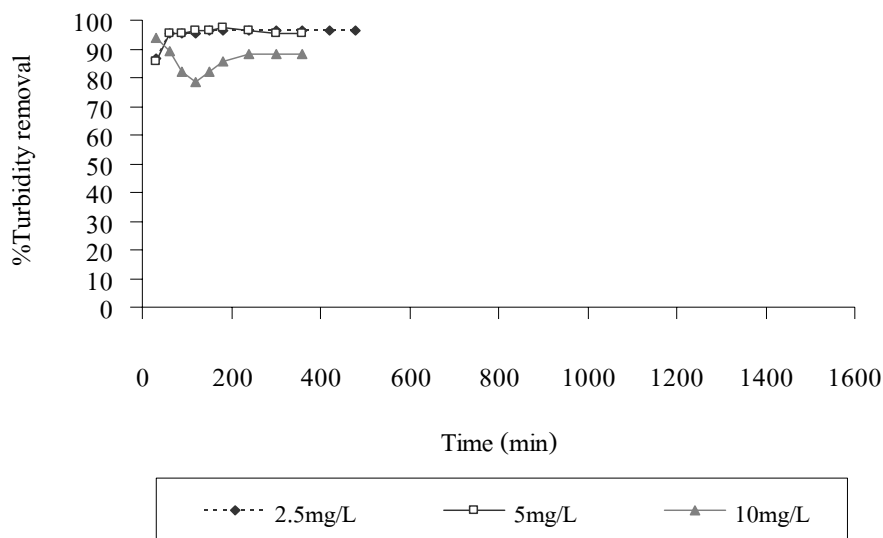


Figure 10 Turbidity removal of the single floating-media (3-mm bead diameter, 60-cm layer depth) flocculator different dosages of PACl under the hydraulic rate of $2.5 \text{ m}^3/\text{m}^2\text{-h}$.

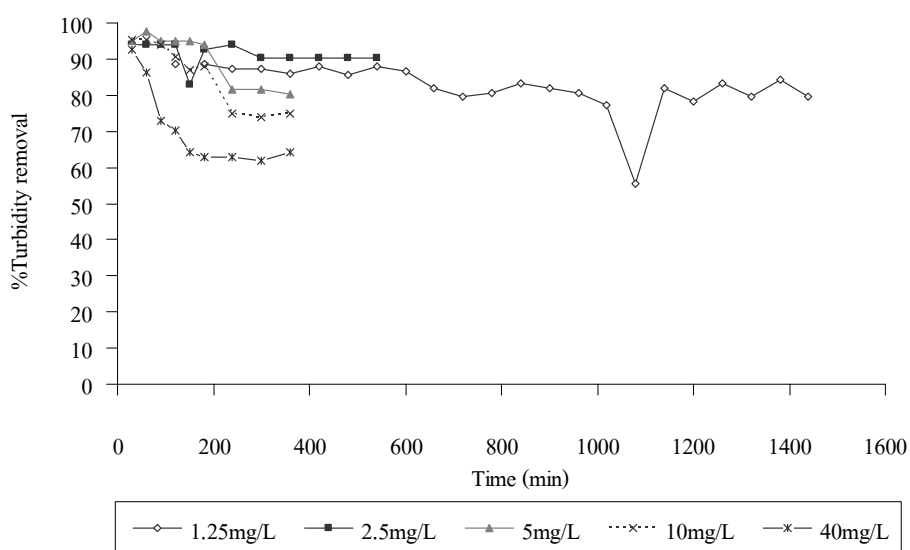


Figure 11 Turbidity removal of single floating-media (3-mm bead diameter, 60-cm layer depth) flocculator different dosages of PACl under the hydraulic rate of $5 \text{ m}^3/\text{m}^2\text{-h}$

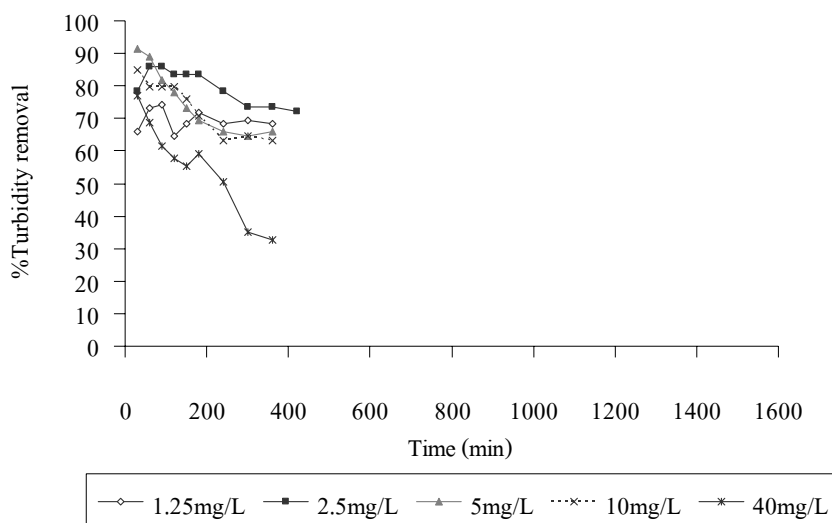


Figure 12 Turbidity removal of single floating-media (3-mm bead diameter, 60-cm layer depth) flocculator different dosages of PACl under the hydraulic rate of $10 \text{ m}^3/\text{m}^2\text{-h}$.

2.1.2 Effect of PACl doses on head loss development

Figures 13-15 represent the performance of system in terms of head loss development different PACl doses of hydraulic rates of $2.5 \text{ m}^3/\text{m}^2\text{-h}$, $5 \text{ m}^3/\text{m}^2\text{-h}$ and $10 \text{ m}^3/\text{m}^2\text{-h}$, respectively. As can be seen in Figure 13, the accumulated head loss development was observed to be very low. The head loss developments found were 10 mm, throughput 0.127 m^3 within 8 hours, 12 mm, throughput 0.095 m^3 within 6 hours and 21 mm, throughput 0.095 m^3 within 6 hours for the experiments using PACl doses of 2.5 mg/L, 5 mg/L and 10 mg/L, respectively. Figure 14 shows similar results, the head loss development was found to be only 52 mm, throughput 0.320 m^3 within 24 hours, 31mm, throughput 0.143 m^3 within 9 hours, 42 mm, throughput 0.095 m^3 within 6 hours, 43 mm, throughput 0.095 m^3 within 6 hours and 65 mm, throughput 0.095 m^3 within 9 hours at PACl doses of 1.25 mg/L, 2.5 mg/L, 5 mg/L, 10 mg/L and 40 mg/L, respectively.

Figure 15, the head loss developments were found to be 37 mm, throughput 0.384 m^3 within 6 hours, 49 mm, throughput 0.448 m^3 within 7 hours, 49 mm, throughput 0.384 m^3 within 6 hours, 52 mm, throughput 0.384 m^3 within 6 hours and 44 mm, throughput 0.384 m^3

within 9 hours at PACl doses of 1.25 mg/L, 2.5 mg/L, 5 mg/L, 10 mg/L and 40 mg/L, respectively. Because of the higher dose led to greater clogging, the flocculation mechanisms in the floating-media column, larger expansion of floating media depth and quicker detachment of flocs from media (Ngo and Vigneswaran, 1995a, 1995b). As can be seen in Figure 15, the head loss development of 40-mg/L PACl dosage was reduced from 55 mm to 41 mm after the media layer expanded about 4 mm. Then, the flocs had started to fall down from the media while the media was expanding. This occurrence caused the deterioration of effluent quality.

Table 6, we can observe the coagulant that the high dosage caused the high head loss development. The floc volume was proportional to the coagulant dosage used. The high dosage resulted in a large volume of flocs and the rapid clogging of the porous media resulting in a shorter operating time (Adin and Rebhun, 1974).

Table 6 Performance of single floating media flocculator at different dosages of PACl and different hydraulic rates (layer depth of 60 cm. and media size of 3 mm)

Run no.	Hydraulic rates ($\text{m}^3/\text{m}^2\cdot\text{h}$)	PACl doses (mg/L)	Average %Tb removal	Head loss development (mm)/ h	Expanded depth (cm)	Average G (s^{-1})	Average floc (Digital camera) (μm)
1	2.5	2.5	95.2	10 mm / 8 hr	0.1	20.4	329
2	2.5	5	94.9	12 mm / 6 hr	0.1	20.4	325
3	2.5	10	86.1	21 mm / 6 hr	0.1	29.8	252
4	5	1.25	82.5	52 mm / 24 hr	0.2	45.7	211
5	5	2.5	91.4	31 mm / 9 hr	0.1	43.5	239
6	5	5	90.5	42 mm / 6 hr	0.1	41.5	222
7	5	10	85.9	43 mm / 6 hr	0.1	42.4	247
8	5	40	70.9	65 mm / 6 hr	0.2	57.8	236
9	10	1.25	69.4	37 mm / 6 hr	0.2	66.7	195
10	10	2.5	79.9	49 mm / 7 hr	0.6	77.4	233
11	10	5	75.5	49 mm / 6 hr	0.2	76.1	323
12	10	10	73.6	52 mm / 6 hr	0.2	76.8	225
13	10	40	35.3	44 mm / 6 hr	0.5	84.9	191

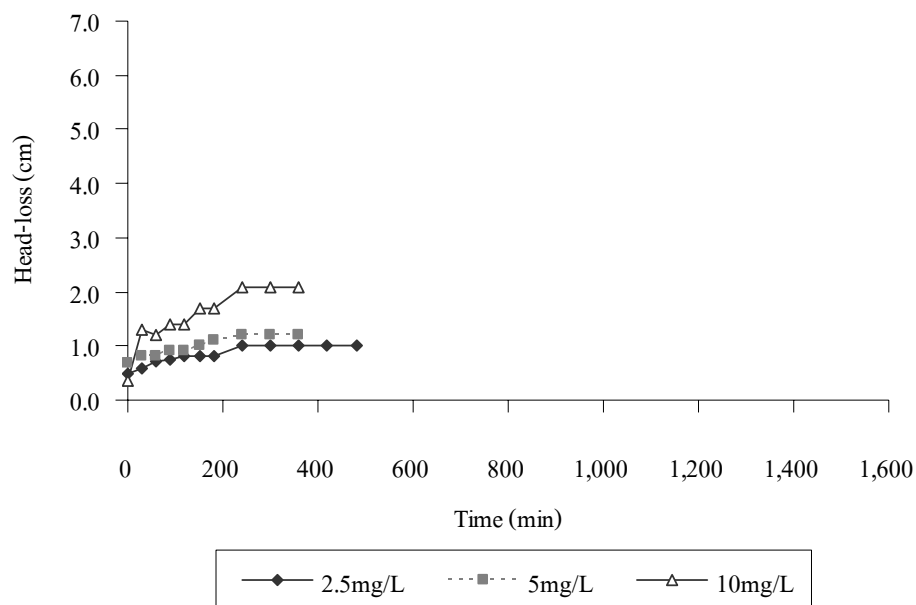


Figure 13 Head-loss development of single floating-media (3-mm bead diameter, 60-cm layer depth) flocculator different doses of PACl under hydraulic rate of $2.5 \text{ m}^3/\text{m}^2\text{-h}$

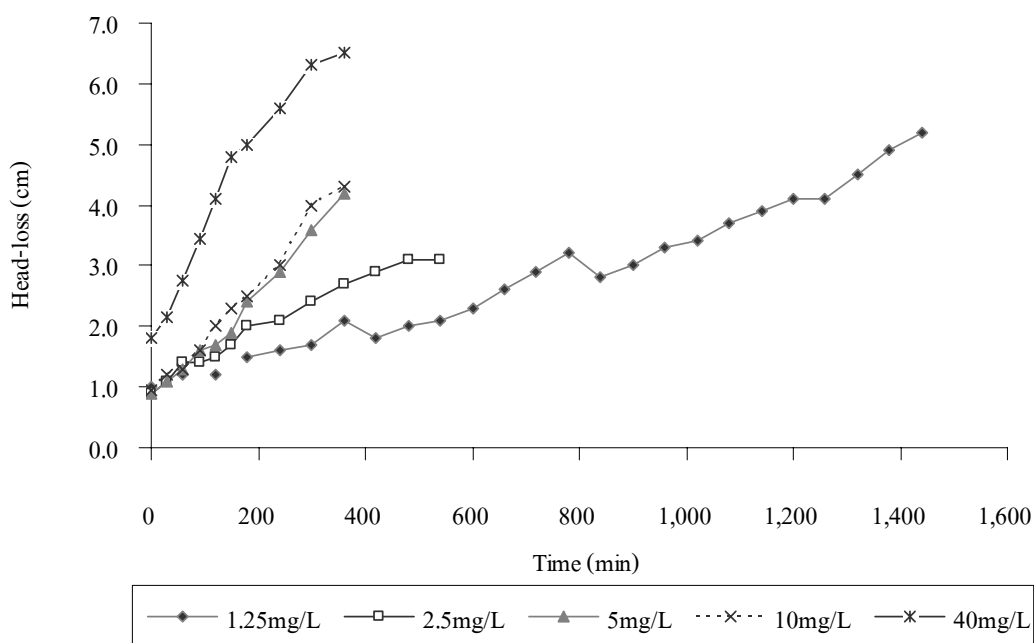


Figure 14 Head-loss development of single floating-media (3-mm bead diameter, 60-cm layer depth) flocculator different dosages of PACl under hydraulic rate of $5 \text{ m}^3/\text{m}^2\text{-h}$.

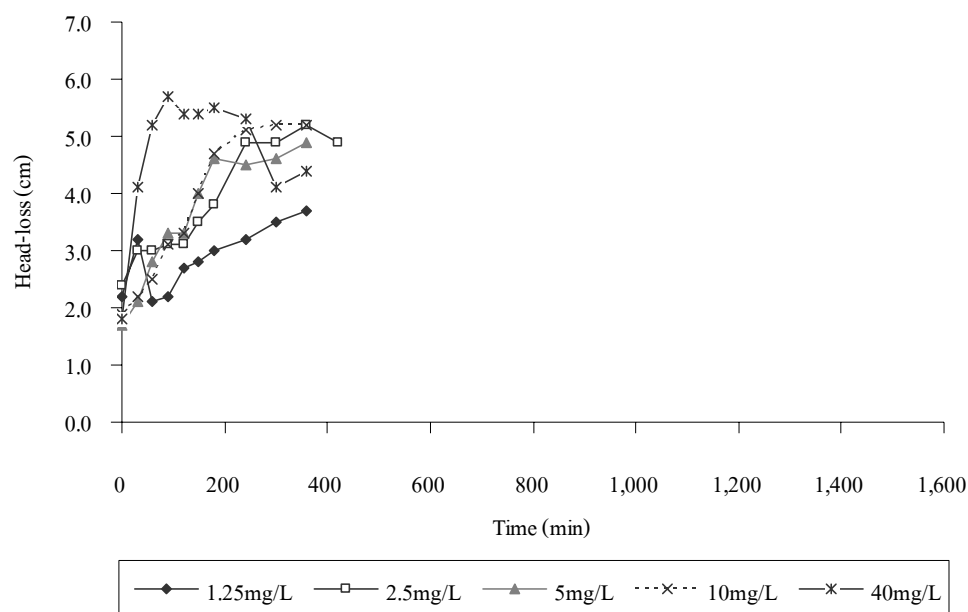


Figure 15 Head-loss development of single floating-media (3-mm bead diameter, 60-cm layer depth) flocculator different dosages of PACl under hydraulic rate of $10 \text{ m}^3/\text{m}^2\text{-h}$.

2.1.3 Effect of PACl doses on average floc size

Figures 16-18 presented the performance of the system in terms of average floc size different PACl doses of hydraulic rates of $2.5 \text{ m}^3/\text{m}^2\text{-h}$, $5 \text{ m}^3/\text{m}^2\text{-h}$ and $10 \text{ m}^3/\text{m}^2\text{-h}$, respectively. Figure 16, the average floc size was examined using digital image analysis. The average floc sizes found were $392 \mu\text{m}$ within 8 hours, $285 \mu\text{m}$ within 6 hours and $253 \mu\text{m}$ within 6 hours for the experiments using PACl doses of 2.5 mg/L , 5 mg/L and 10 mg/L , respectively. Figure 17 shows similar results, the average floc size was found to be $172 \mu\text{m}$ within 24 hours, $239 \mu\text{m}$ within 9 hours, $222 \mu\text{m}$ within 6 hours, $248 \mu\text{m}$ within 6 hours and $237 \mu\text{m}$ within 9 hours at PACl doses of 1.25 mg/L , 2.5 mg/L , 5 mg/L , 10 mg/L and 40 mg/L , respectively. Figure 18 shows the average floc size were found to be $195 \mu\text{m}$ within 6 hours, $233 \mu\text{m}$ within 7 hours, $223 \mu\text{m}$ within 6 hours, $225 \mu\text{m}$ within 6 hours, and $191 \mu\text{m}$ within 6 hours at PACl doses of 1.25 mg/L , 2.5 mg/L , 5 mg/L , 10 mg/L and 40 mg/L , respectively.

Figures 16 and 18 could observe that the flocculent dose that any flocculent dosage caused the average floc size continue to increase in size with operation time. Figure 17, at a hydraulic rate of $5 \text{ m}^3/\text{m}^2\text{-h}$, PACl dose of 1.25 mg/L, the average floc sizes continue to increase until steady-state average floc size started at 600 minutes. Figures 16-18, the whole average floc size shifts progressively to larger floc with increasing PACl dosage, when dose $\leq 2.5 \text{ mg/L}$, beyond 2.5 mg/L the average floc sizes become smaller floc and insensitive to further increase in PACl dose.

Table 6 summarized the experimental results obtained at different hydraulic rates and PACl doses. From Table 5, PACl dose of 2.5 mg/L provided the highest average turbidity removal percent of 95.2, 91.4 and 79.8 at hydraulic rates of 2.5, 5 and $10 \text{ m}^3/\text{m}^2\text{-h}$, respectively. The maximum average floc produced from floating media flocculator at 2.5 mg/L PACl also yielded the biggest size of 393, 340, 255 at hydraulic rates of 2.5, 5 and $10 \text{ m}^3/\text{m}^2\text{-h}$. It should be note that the optimum dose of system was 2.5 mg/L of PACl .

From the experiment, the optimum coagulant dose in floating media column was 2.5 mg/L. The flocculation in floating media column required low coagulant dosage. It was because that the floating-media column performed similar to a contact flocculator which promoted the change in velocity gradient along the flow direction, so called “tapered flocculation”. The bigger-formed flocs can penetrate through the void of media. Subsequently, the collision between flocs in the void of media promoted the larger flocs (Culp, 1977; Luttinger, 1981 and Kludpiban, 2000). Moreover, the overdosing of coagulant (10 mg/L) could result in media clogging, rapid head-loss development and turbidity breakthrough. Finally, the poor effluent water quality was produced. On the other hand, if the coagulant dosage was too low, the chemical coagulation-flocculation would not be completed the resulting the high turbidity of effluent water.

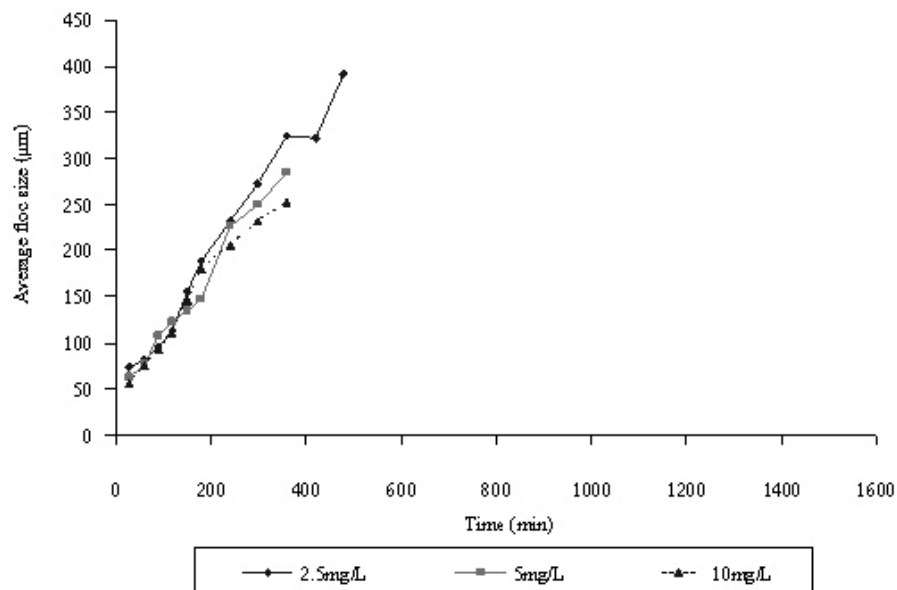


Figure 16 Average floc size of single floating-media (3-mm bead diameter, 60-cm layer depth) flocculator different dosages of PACl under the hydraulic rate of $2.5 \text{ m}^3/\text{m}^2\text{-h}$.

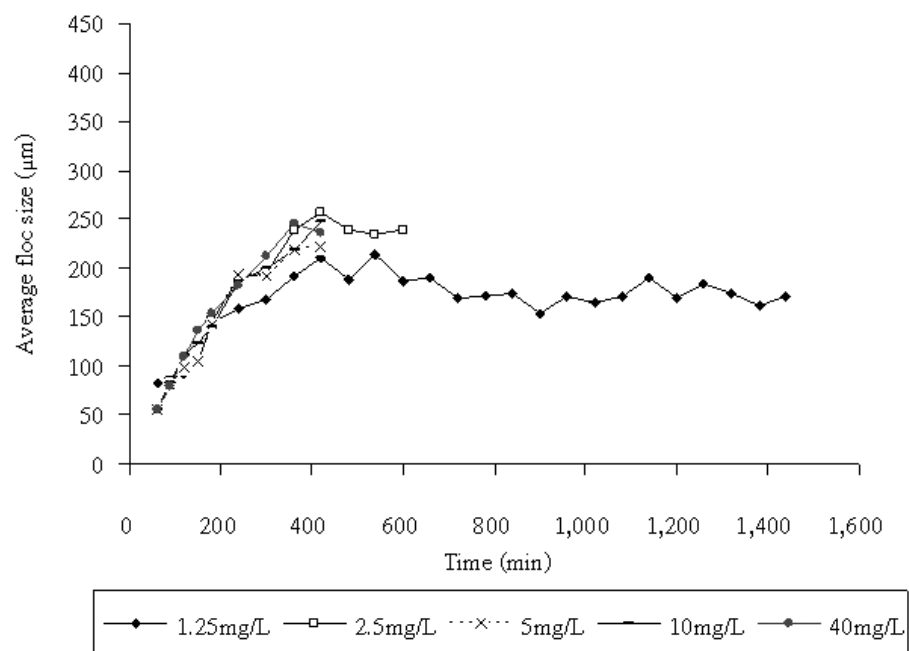


Figure 17 Average floc size of single floating-media (3-mm bead diameter, 60-cm layer depth) flocculator different dosages of PACl under the hydraulic rate of $5 \text{ m}^3/\text{m}^2\text{-h}$.

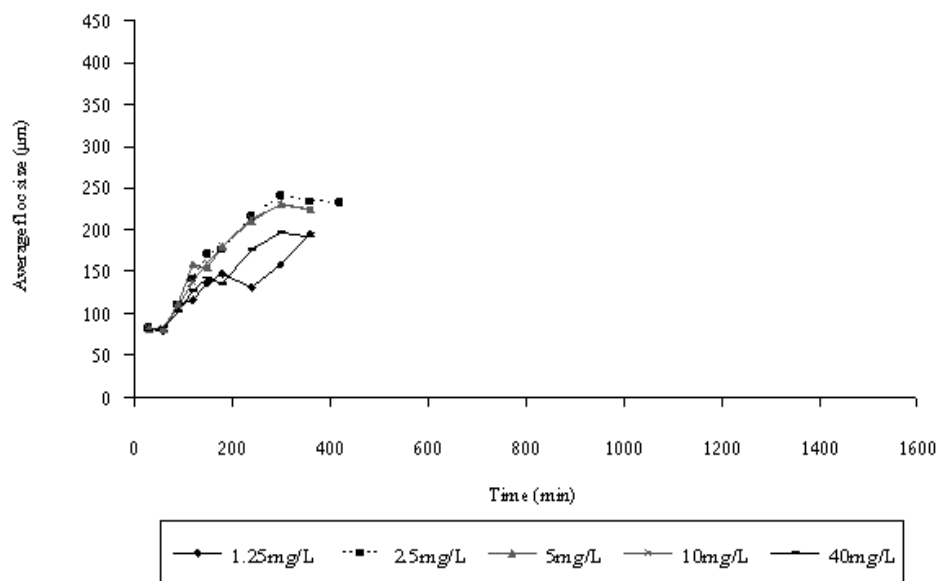


Figure 18 Average floc size of single floating-media (3-mm bead diameter, 60-cm layer depth) flocculator different dosages of PACl under the hydraulic rate of $10 \text{ m}^3/\text{m}^2\text{-h}$.

2.2 Effect of hydraulic rates

2.2.1 Effect of hydraulic rates on turbidity removal percent

Figures 19-23 illustrate the performance of the system in terms of turbidity removal with different hydraulic rates and different PACl doses of 1.25 mg/L, 2.5 mg/L, 5 mg/L, 10 mg/L and 40 mg/L. From Figure 19, the average turbidity removals were 82.5% and 69.4% at the hydraulic rates of $5 \text{ m}^3/\text{m}^2\text{-h}$ and $10 \text{ m}^3/\text{m}^2\text{-h}$, respectively. Figure 20 shows the average turbidity removals were 95.2%, 91.4% and 79.9% at the hydraulic rates of $2.5 \text{ m}^3/\text{m}^2\text{-h}$, $5 \text{ m}^3/\text{m}^2\text{-h}$ and $10 \text{ m}^3/\text{m}^2\text{-h}$, respectively. Figure 21 shows the average turbidity removals were 90.5%, 75.5%, and 69.4% at the hydraulic rates of $2.5 \text{ m}^3/\text{m}^2\text{-h}$, $5 \text{ m}^3/\text{m}^2\text{-h}$ and $10 \text{ m}^3/\text{m}^2\text{-h}$, respectively. Figure 22 shows the average turbidity removals were 86.1%, 85.9% and 73.6% at the hydraulic rates of $2.5 \text{ m}^3/\text{m}^2\text{-h}$, $5 \text{ m}^3/\text{m}^2\text{-h}$ and $10 \text{ m}^3/\text{m}^2\text{-h}$, respectively. Figure 23 shows the average turbidity removals were 70.9% and 35.3% at the hydraulic rates of $5 \text{ m}^3/\text{m}^2\text{-h}$ and $10 \text{ m}^3/\text{m}^2\text{-h}$, respectively.

Figures 19-23, indicate an increase in hydraulic rate reduced effluent water quality in term of decreasing turbidity removal efficiency (in percentage). It was observed that application of hydraulic rate at $2.5 \text{ m}^3/\text{m}^2\text{-h}$ could produce the highest turbidity removal for any coagulant dose. From Table 4, the highest average turbidity removals at the hydraulic rate of $2.5 \text{ m}^3/\text{m}^2\text{-h}$ were 95.2%, 94.9%, and 86.1% with the PACl doses of 2.5 mg/L, 5 mg/L, and 10 mg/L, respectively.

Increasing the hydraulic rate increased the floc rate deposit on the floating beads. This had an additional effect of increasing the interpore shear forces. If the shear forces exceeded the attachment forces, floc could push from the surface of media prior to capture. The net result was the reduction in effluent quality.

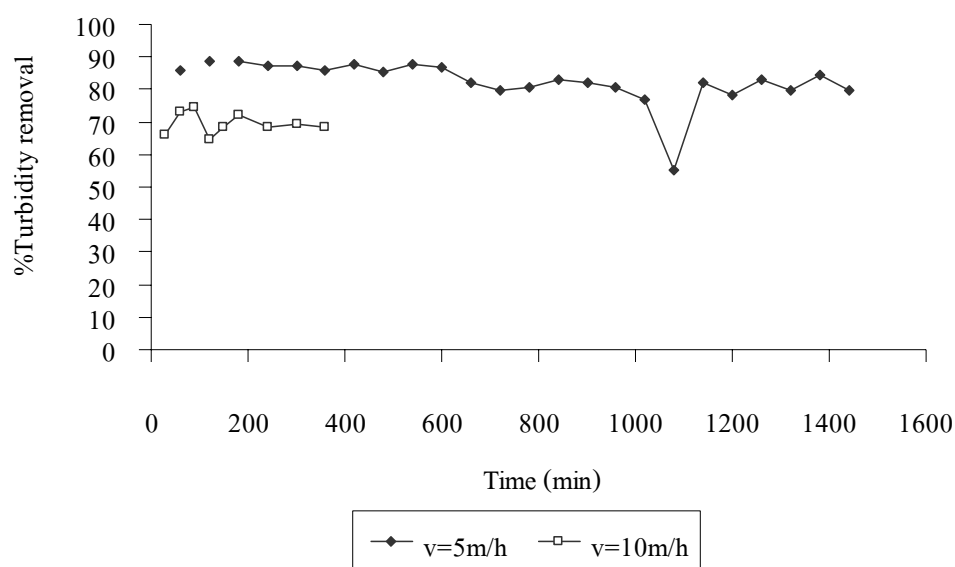


Figure 19 Turbidity removal of single floating-media (3-mm bead diameter, 60-cm depth) flocculator different hydraulic rate on PACl dose of 1.25 mg/L

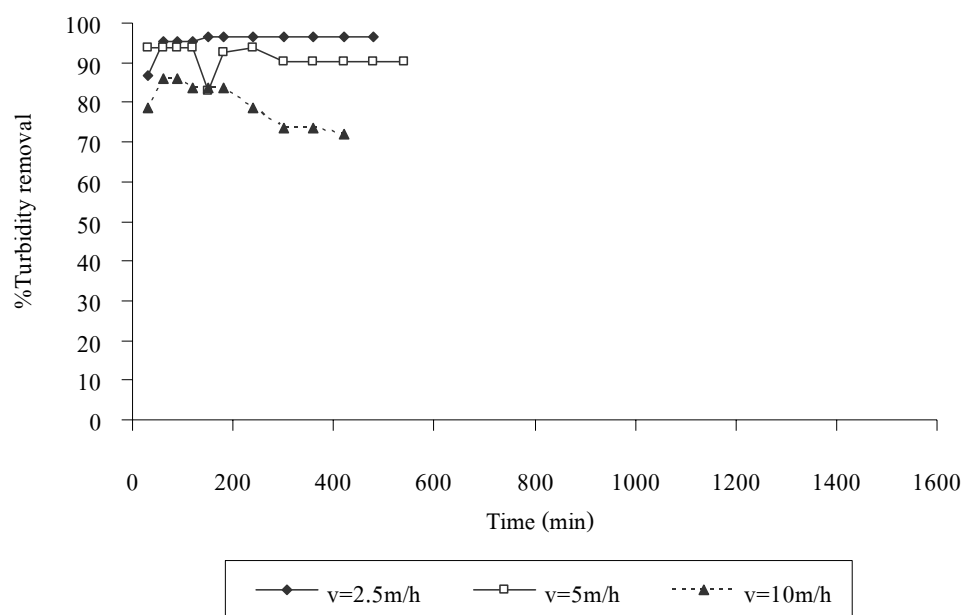


Figure 20 Turbidity removal of single floating-media (3-mm bead diameter, 60-cm depth) flocculator different hydraulic rates on PACl dose of 2.5 mg/L

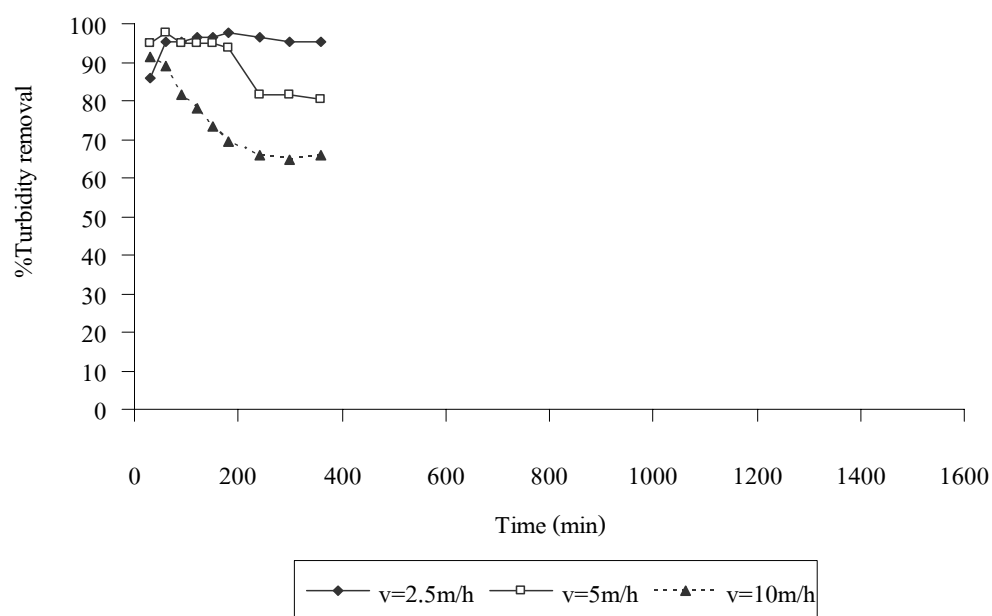


Figure 21 Turbidity removal of single floating-media (3-mm bead diameter, 60-cm depth) flocculator different hydraulic rates on PACl dose of 5 mg/L

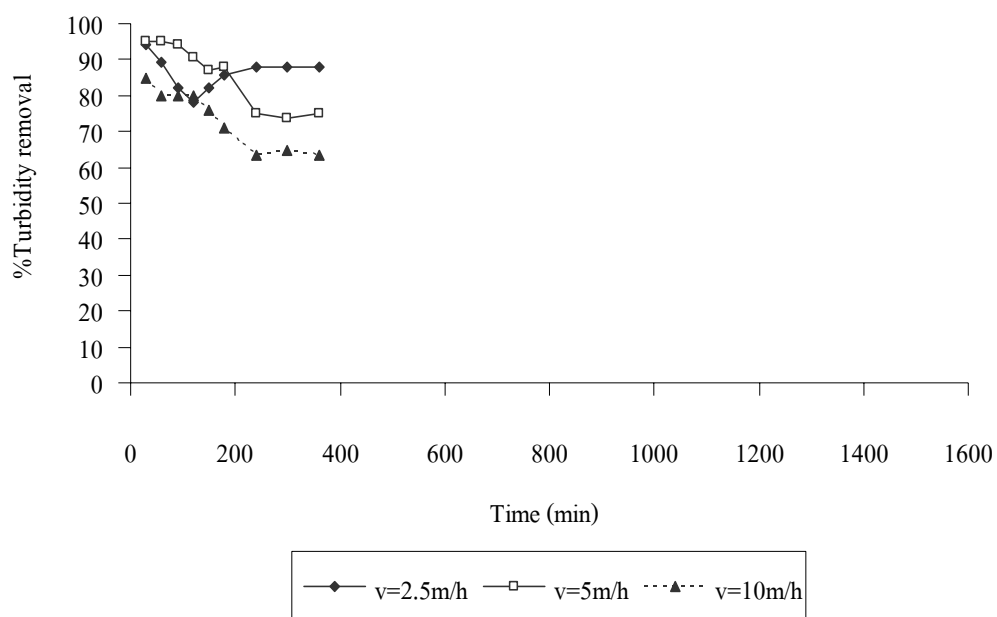


Figure 22 Turbidity removal of single floating-media (3-mm bead diameter, 60-cm depth) flocculator different hydraulic rates on PACl dose of 10 mg/L

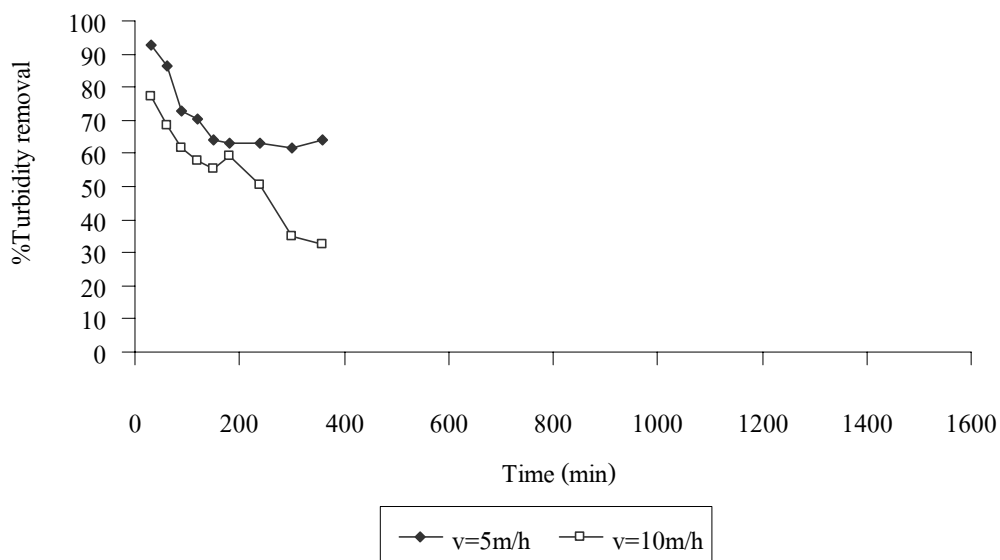


Figure 23 Turbidity removal of single floating-media (3-mm bead diameter, 60-cm depth) flocculator different hydraulic rates on PACl dose of 40 mg/L

2.2.2 Effect of hydraulic rates on head loss development

The comparison between the accumulated head loss development with the same dosages of PACl (1.25 mg/L, 2.5 mg/L, 5 mg/L, 10 mg/L, and 40 mg/L), but different hydraulic rates are shown in Figures 24-28. As shown in Figure 28, the head loss developments were observed to be 65 mm, throughput 0.192 m^3 within 6 hours and 44 mm, throughput 0.384 m^3 within 6 hours at the hydraulic rates of $5 \text{ m}^3/\text{m}^2\text{-h}$ and $10 \text{ m}^3/\text{m}^2\text{-h}$, respectively. As mentioned before, the head loss development of 40-mg/L PACl dosage under the hydraulic rate of $10 \text{ m}^3/\text{m}^2\text{-h}$ reduced from 55 mm to 41 mm because of bed expansion.

Figure 24, the head loss developments were found to be 10 mm, throughput 0.129 m^3 within 8 hours, 31 mm, throughput 0.256 m^3 within 9 hours and 49 mm, throughput 0.450 m^3 within 7 hours at the hydraulic rates of $2.5 \text{ m}^3/\text{m}^2\text{-h}$, $5 \text{ m}^3/\text{m}^2\text{-h}$ and $10 \text{ m}^3/\text{m}^2\text{-h}$, respectively. The result showed that higher hydraulic rates provided higher head loss development for all PACl doses because the head loss was the function of floc volume retained in bed, cross-section area bed, media size and flow rate (O'Melia and Ali, 1978). The higher rate increased the rate of retained-floc volume and head loss accumulation until it reached the point that bed expanded. The floc pulled down from the bed resulting in lower head loss. The same results were also found in Figures 24-28.

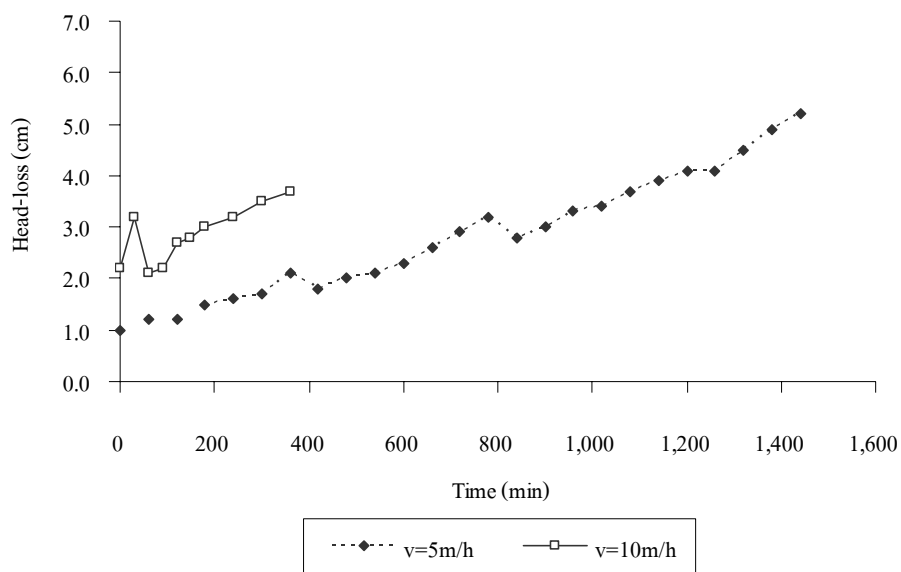


Figure 24 Head-loss development of single floating-media (3-mm bead diameter, 60-cm layer depth) flocculator different hydraulic rates on dose of PACl of 1.25 mg/L

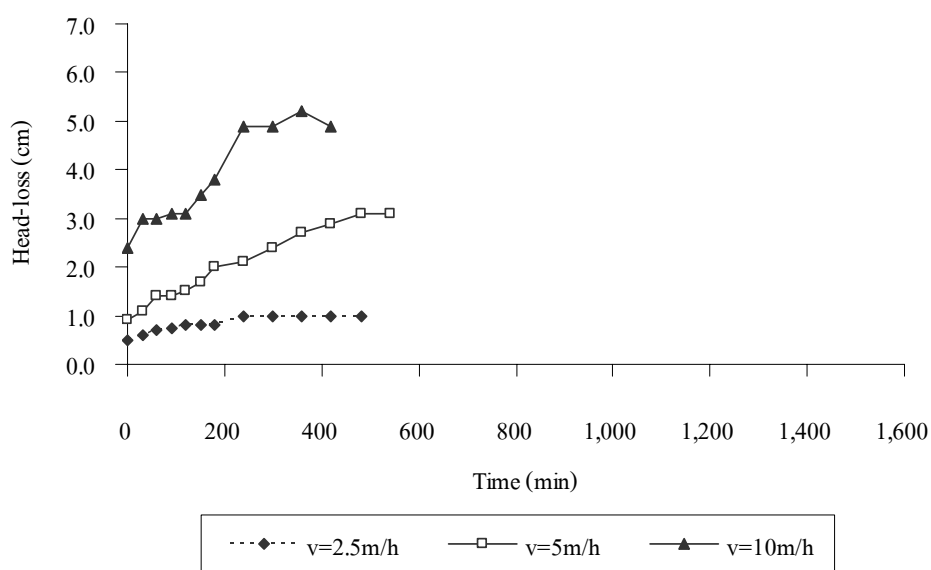


Figure 25 Head-loss development of single floating-media (3-mm bead diameter, 60-cm layer depth) flocculator different hydraulic rates on dose of PACl of 2.5 mg/L

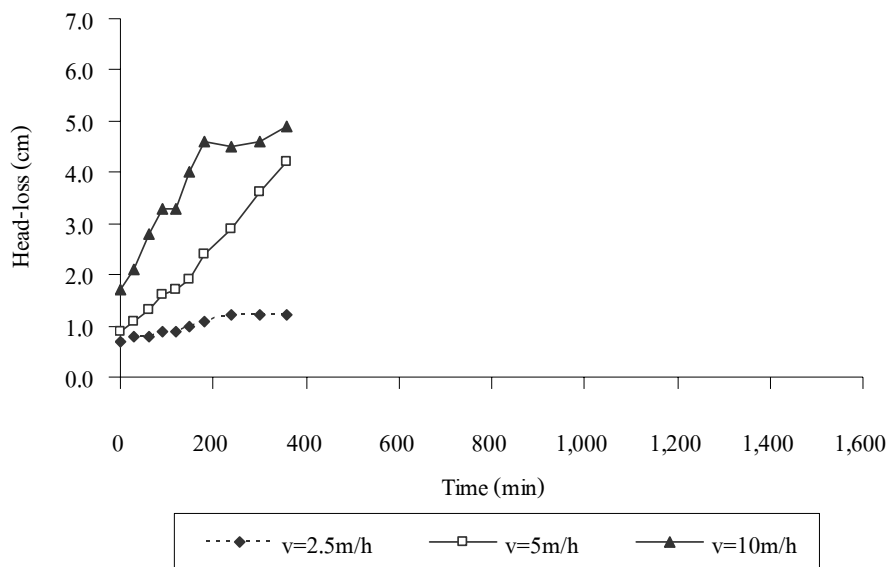


Figure 26 Head-loss development of single floating-media (3-mm bead diameter, 60-cm layer depth) flocculator different hydraulic rates on dose of PACl of 5 mg/L

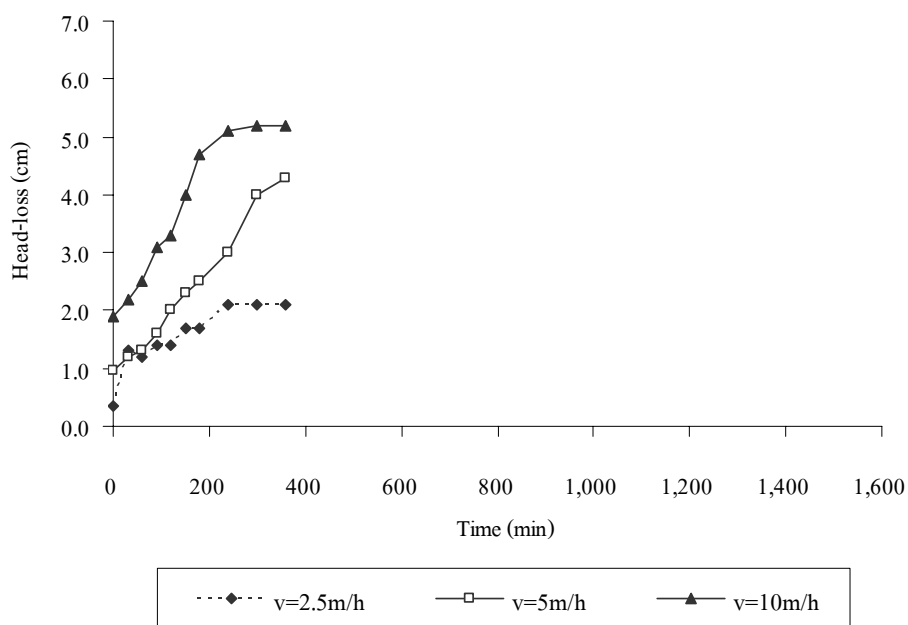


Figure 27 Head-loss development of single floating-media (3-mm bead diameter, 60-cm layer depth) flocculator different hydraulic rates on dose of PACl of 10 mg/L

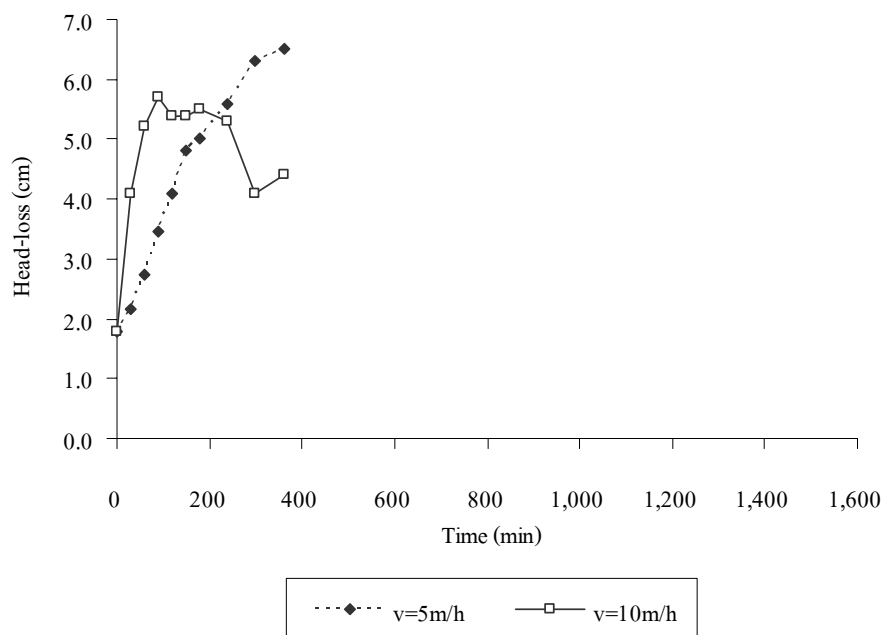


Figure 28 Head-loss development of single floating-media (3-mm bead diameter, 60-cm layer depth) flocculator different hydraulic rates on dose of PACl of 40 mg/L

2.2.3 Effect of hydraulic rates on average floc size

Figures 29-33 presented the performance of the system in terms of average floc size different hydraulic rates of PACl doses of 21.25 mg/L, 2.5 mg/L, 5 mg/L, 10 mg/L, and 40 mg/L, respectively. Figure 29, the average floc size was observed to be 172 μm within 24 hours and 195 μm within 6 hours at PACl dosage of 1.25 mg/L, the hydraulic rates of 5 $\text{m}^3/\text{m}^2\text{-h}$ and 10 $\text{m}^3/\text{m}^2\text{-h}$, respectively. The average floc size was a function of floc formation of the system. The result showed that higher hydraulic rates provided lower average floc size at the same PACl dose. The higher hydraulic rate decreased the floc formation to promote flocculent-floc. The same results were also found in Figures 29-33.

As mentioned above, the velocity gradient was dictated by head-loss. The head-loss was a function of flow rate. Shear forces due to too high velocity gradient could break up larger floc and limit the maximum floc size. Consequently, the high hydraulic rate produced the

high velocity gradient resulting in decreasing of maximum floc size. From Table 5, the average floc size decreased with increasing in hydraulic rate (same PACl dose).

The experiments to select optimum hydraulic rate and PACl dose were carried out using $2.5 \text{ m}^3/\text{m}^2\cdot\text{h}$ and 2.5 mg/L , respectively. The optimum hydraulic rate and PACl dose were selected because these conditions yielded the highest average turbidity removal percent of 95.2, the lowest head-loss development of 10 mm within 8 hours, average floc size also yielded the biggest size of $329 \text{ }\mu\text{m}$.

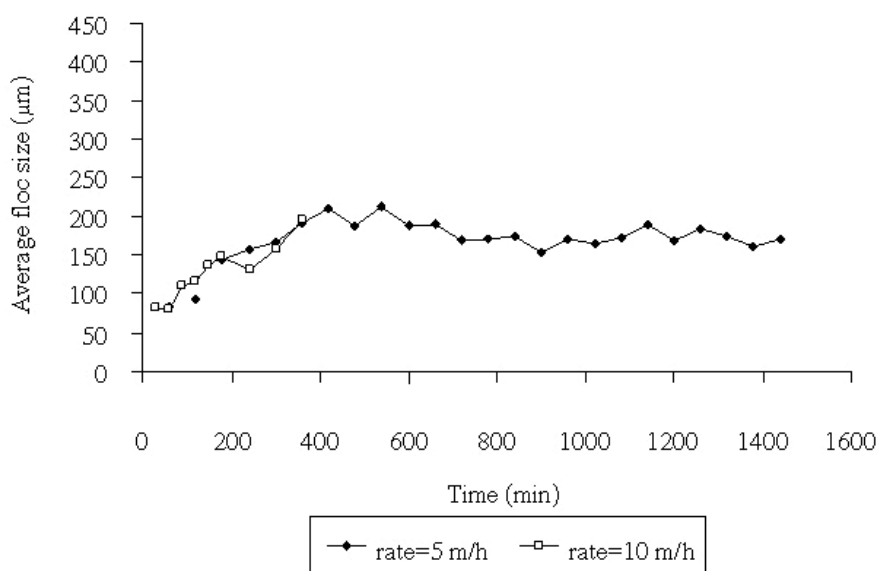


Figure 29 Average floc size of single floating-media (3-mm bead diameter, 60-cm layer depth) flocculator different hydraulic rates on dose of PACl of 1.25 mg/L

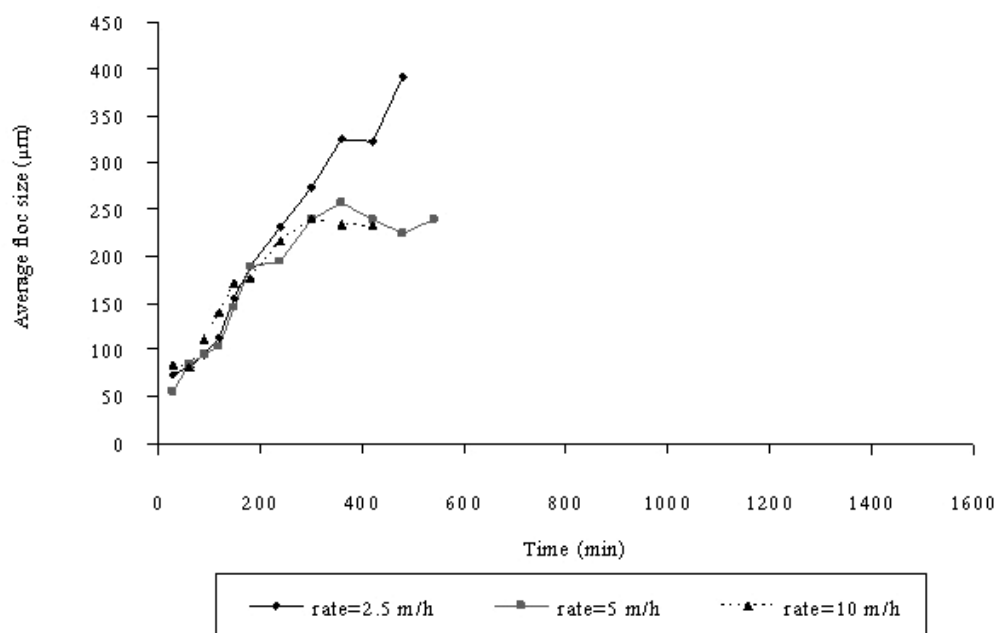


Figure 30 Average floc size of single floating-media (3-mm bead diameter, 60-cm layer depth) flocculator different hydraulic rates on dose of PACl of 2.5 mg/L

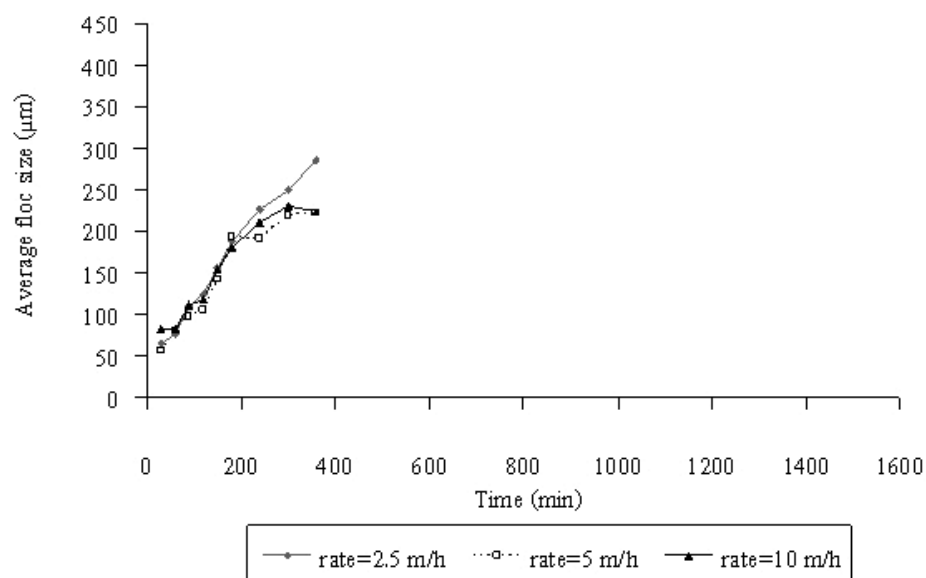


Figure 31 Average floc size of single floating-media (3-mm bead diameter, 60-cm layer depth) flocculator different hydraulic rates on dose of PACl of 5 mg/L

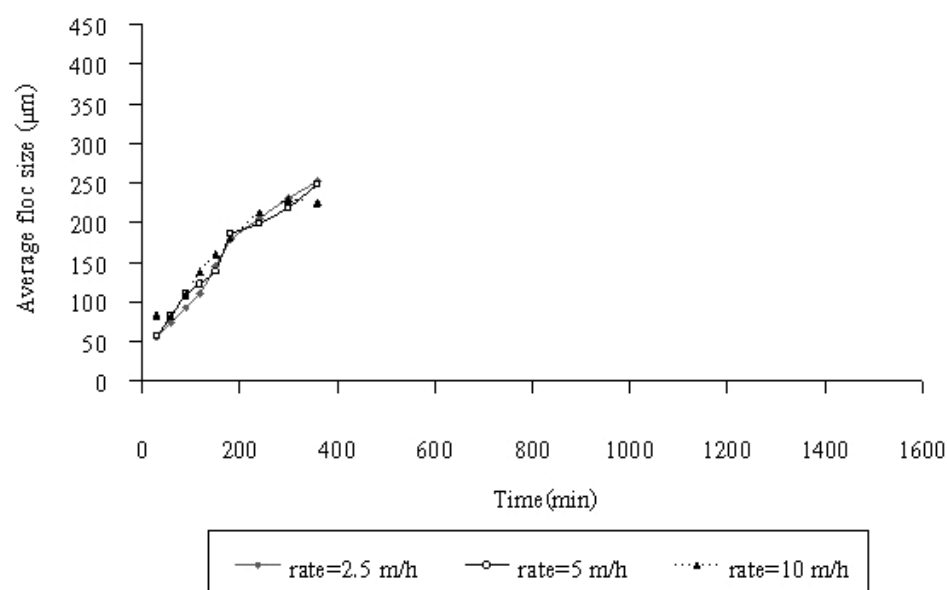


Figure 32 Average floc size of single floating-media (3-mm bead diameter, 60-cm layer depth) flocculator different hydraulic rates on dose of PACl of 10 mg/L

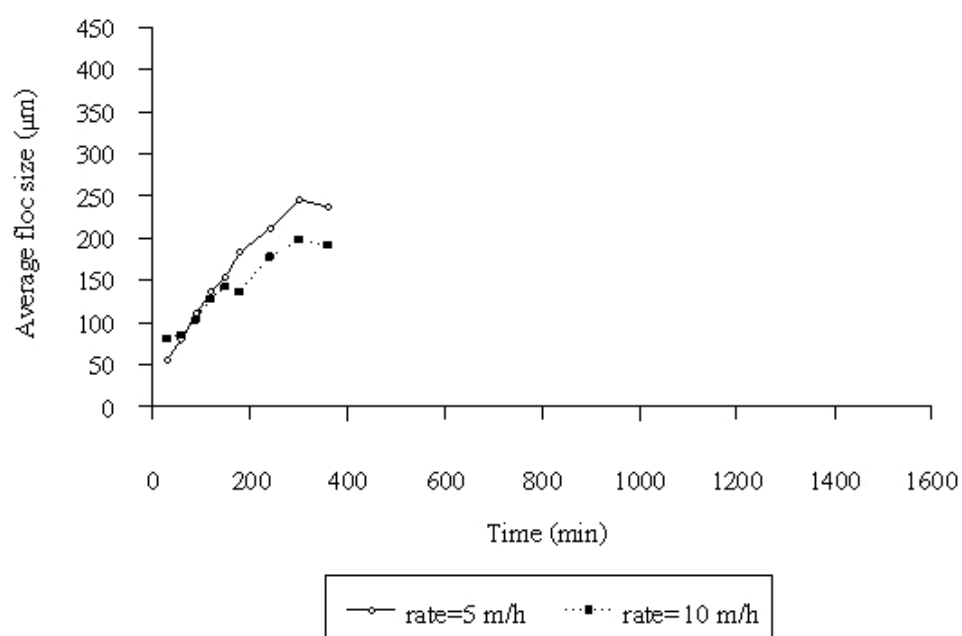


Figure 33 Average floc size of single floating-media (3-mm bead diameter, 60-cm layer depth) flocculator different hydraulic rates on dose of PACl of 40 mg/L

3. Performance of floating plastic media flocculator

This study was done by applying a floating media of polypropylene beads with a diameter of about 3-mm, 6-mm and 10-mm. The floating-media flocculator was operated as single, dual and multilayer configuration at the layer depth of 30-cm and 60-cm. The performance of the floating-media flocculator was examined using the optimum conditions obtained from experimental run no.1-13 (influent turbidity of 80 NTU, 2.5 mg/L of PACl dose and hydraulic rate of $2.5 \text{ m}^3/\text{m}^2\text{-h}$).

The head-loss developments with different media sizes at the hydraulic rate $2.5 \text{ m}^3/\text{m}^2\text{-h}$ were illustrated in Table 6. The smaller media resulted in the higher head-loss development. The head-loss was caused by the accumulation of flocs within media bed (O'Melia and Ali, 1978), the head-loss was the functions of floc size and pore size. Therefore, the smaller media pore size would greater effect on the head-loss development. From Table 7, the accumulated head-losses were 9 mm, 3 mm and 2 mm with media sizes of 3-mm, 6-mm and 10-mm, respectively.

The average floc sizes were $336 \mu\text{m}$, $354 \mu\text{m}$ and $376 \mu\text{m}$ with the media sizes of 3 mm, 6 mm and 10 mm, respectively. As mentioned before, the velocity gradient was proportional to head-loss development. The smaller media size yielded the higher head-loss development. Consequently, the smaller size of media also yielded the higher velocity gradient resulting in decreasing of maximum floc size. The overall results could be concluded that the increase of media size resulted in the decrease of head-loss development and the increase of average maximum floc size.

The overall performance of single and multilayer floating-media flocculator was considered. Figures 34-35 demonstrate that the smallest single media produced the highest head-loss and smallest average floc size (3-mm in diameter). Whilst the biggest single media produced the lowest head-loss and the biggest maximum floc size (10-mm in diameter). From Table 5, the multilayer-floating-media yielded the same trend of results. The multilayer-floating-media produced bigger floc when compared with the smaller single media because of the grading size of

media resulting in tapered flocculation. The multilayer floating media decreased head-loss when compared with the smaller single media because this system allowed fine floc to penetrate deeper into the coarse media and more area of media was utilized.

The longer media depth produced longer detention time in bed resulting in higher *GT* or Camp number. The higher *GT* yielded the smaller maximum floc size when compared at the same size of media. However, the changes in parameter *GT* were not corresponding to the changes in floc size when the different media sizes were applied. Therefore, the next study should be study the other parameter that effected on floc size excepting *GT*. It could be concluded that the bigger size and shorter depth of media succeeded in producing bigger floc formation and lower head-loss development.

Table 7 Performance of single, dual, and multilayer floating media system

Run no.	Media size (mm)			layer depth (cm)	Velocity gradient (s ⁻¹); G	Detention time in media (s); T	GT	Accumulate headloss (cm)	Average floc size (μm); dS
14	3	-	-	30	21.7	147	3188	0.9	336
15	3	-	-	60	22.4	294	6573	1.1	226
16	6	-	-	30	13.3	156	2073	0.3	354
17	6	-	-	60	14	311	4365	0.4	240
18	10	-	-	30	11	173	1908	0.2	376
19	10	-	-	60	11.5	346	3960	0.4	286
20	3	6	-	30	16.6	151	2518	0.4	264
21	3	6	-	60	17.3	302	5234	0.8	197
22	3	10	-	60	16.9	160	2702	0.6	199
23	3	10	-	60	17.7	320	5662	0.9	134
24	6	10	-	30	13.3	164	2177	0.25	344
25	6	10	-	60	13.6	328	4470	0.5	209
26	3	6	10	30	15.8	158	2496	0.4	315
27	3	6	10	60	16	317	5080	0.7	243

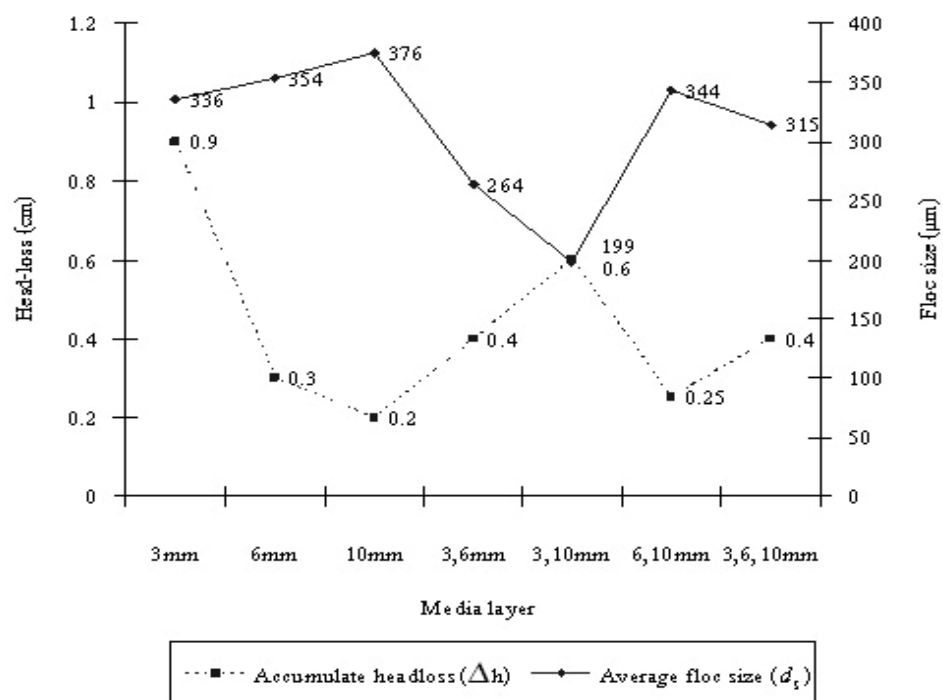


Figure 34 Performance of single and multilayer floating media at layer depth of 30 cm under hydraulic rate of $2.5 \text{ m}^3/\text{m}^2\text{-h}$ and PACl dose of 2.5 mg/L

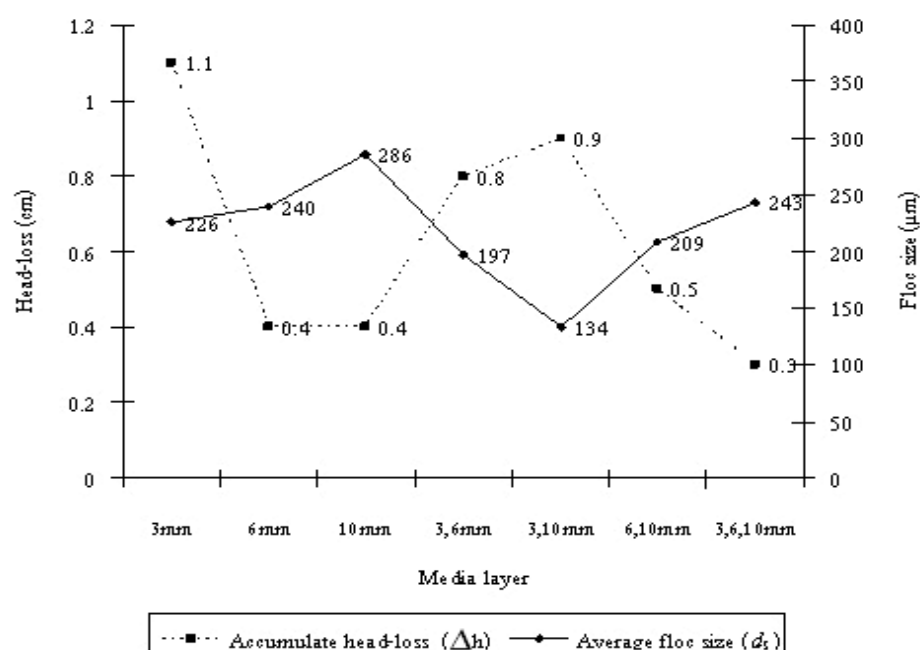


Figure 35 Performance of single and multilayer floating media at layer depth of 60 cm under hydraulic rate of $2.5 \text{ m}^3/\text{m}^2\text{-h}$ and PACl dose of 2.5 mg/L

4. Maximum flocs size (d_M) was observed by using a microscopic analysis

The resolution of microscopic technique was observed flocculent-flocs. A resolution microscope (CHS/CHT, Olympus) at 40X magnification was used to observe. For 10X magnification, it was difficult to measure the number and size of flocs because the flocs size was too small in 10X magnification. For 100X and 400X magnifications, which number and size of flocs were too large and needed too much time to observe. The maximum flocs size (d_M) was observed by using microscopic technique. Samples were taken by inserting a silicone tube (0.5 cm in diameter) in the middle of the column, covering the end by valve, and withdrawing carefully. The flocs were carried out by placing a drop on a glass microscope slide without a cover slip.

The performance of the system in terms of the maximum floc size was observed by using classical techniques. The system was under hydraulic rate of $2.5 \text{ m}^3/\text{m}^2\text{-h}$ and PACl dose of 2.5 mg/L difference media size 3-mm, 6-mm, and 10-mm. The floating-media flocculator was operated as single, dual and multilayer configuration at the layer depth of 30-cm and 60-cm. From Figure 36, the maximum floc size was found to be 65 μm , 25 μm , and 90 μm within 6 hours media size 3-mm, 6-mm, and 10-mm, respectively. Figure 37, the condition same as Figure 36, but except layer depth was 60-cm from 30-cm. The maximum floc size was found to be 65 μm , 15 μm , and 70 μm within 6 hours, respectively. The experimental result of the maximum floc sizes form Figure 38 was found to be 85 μm , 40 μm , and 45 μm within 6 hours difference dual-layer-floating-media of 3,6 mm, 3,10 mm, and 6,10 mm, respectively. Figure 39, the maximum floc sizes was 65 μm , 45 μm , and 30 μm within 6 hours. Figure 40 was multilayer-floating-media of media bead 3 sizes (3-mm, 6-mm, and 10-mm) to be arranged in order of size. Layer depth of 30-cm and 60-cm, maximum floc sizes within 6 hours that are the same were 35 μm .

The performance of the floating media flocculator was examined by using microscopy. A layer depth of 30 cm can form the maximum floc size larger than that formed by a layer depth of 60 cm. This is because higher layer depth and high velocity gradient could break up flocculent-floc size more easily than shorter layer depth. Higher velocity gradient resulted in decreasing of

the flocculent-floc size. Floc breakage occurred during passage through the orifice, where there may be very high shear rates (Gregory, 1998). There is two ways of floc rupture. Small-scale is surface erosion, erosion is due to the shear force act with floc surface resulting in an increase in the small floc size ranges. Large-scale is fragmentation, that is thought to occur from tensile stress acting normally across the whole floc (Jarvisa, 2005).

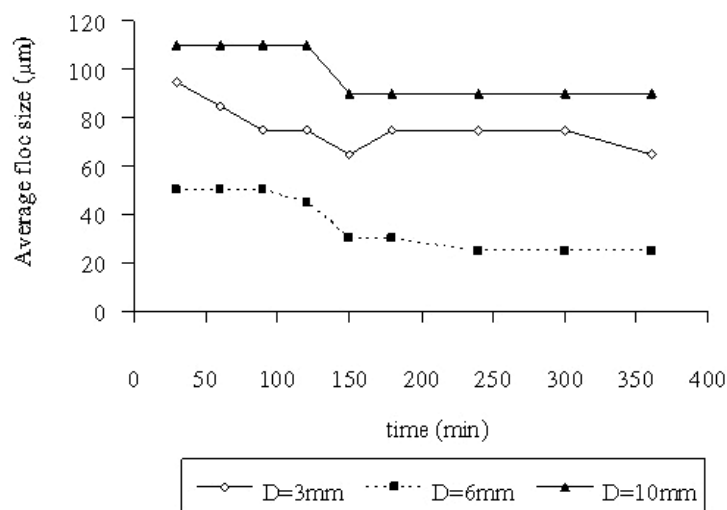


Figure 36 Average maximum floc size of single floating-media difference media size (PACl of 2.5 mg/L, hydraulic rate of $2.5 \text{ m}^3/\text{m}^2\text{-h}$, layer depth of 30-cm)

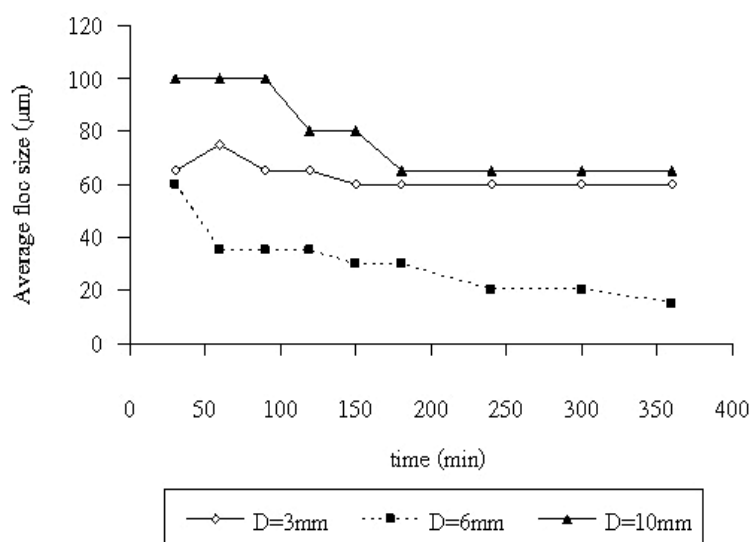


Figure 37 Average maximum floc size of single floating-media difference media (PACl of 2.5 mg/L, hydraulic rate of $2.5 \text{ m}^3/\text{m}^2\text{-h}$, layer depth of 60-cm)

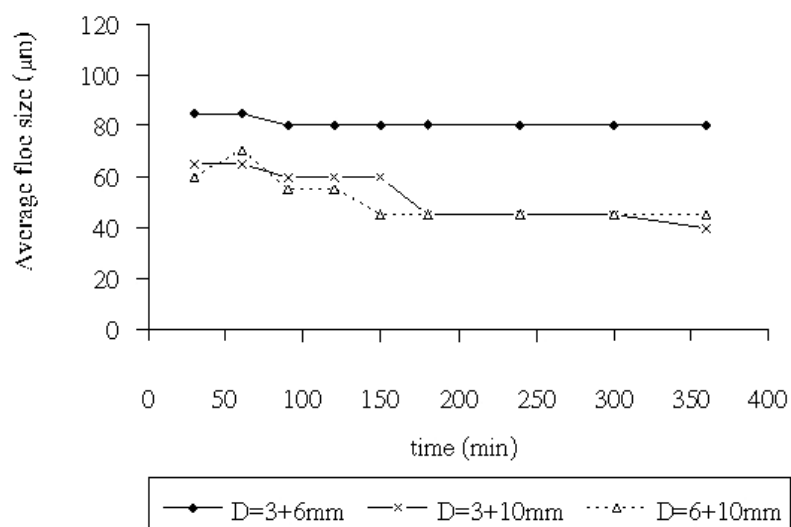


Figure 38 Average maximum floc size of dual-layer floating-media (PACl of 2.5 mg/, hydraulic rate of $2.5 \text{ m}^3/\text{m}^2\text{-h}$, 30-cm layer depth) flocculator different size of medium

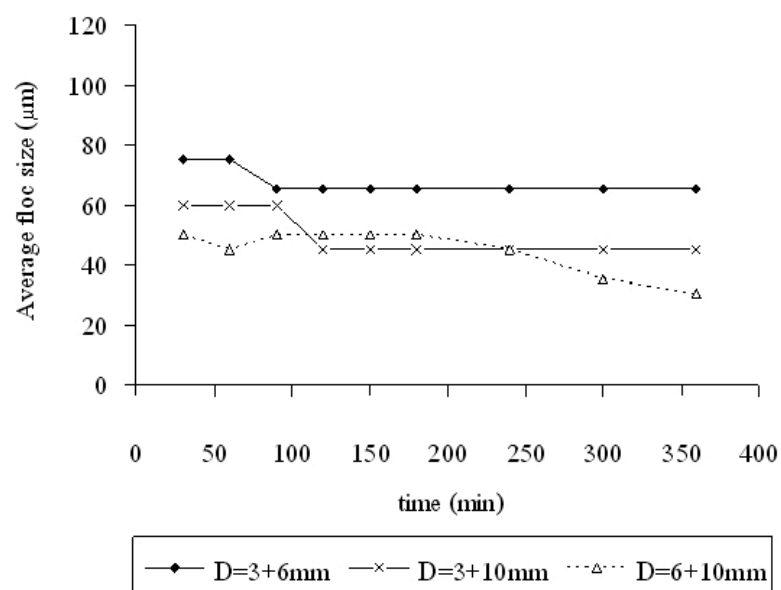


Figure 39 Average maximum floc size of dual-layer floating-media (PACl of 2.5 mg/, hydraulic rate of $2.5 \text{ m}^3/\text{m}^2\text{-h}$, 60-cm layer depth) flocculator different size of medium

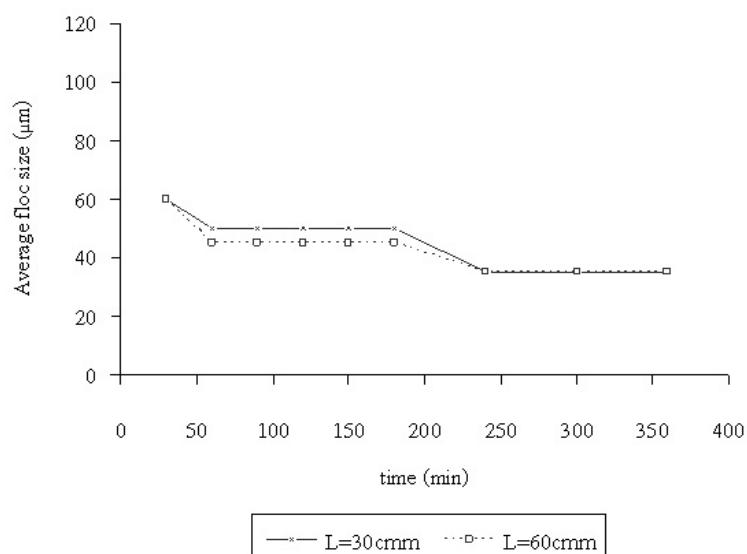


Figure 40 Average maximum floc size of multilayer-floating-media (PACl of 2.5 mg/L, hydraulic rate of $2.5 \text{ m}^3/\text{m}^2\text{-h}$) flocculator different size of medium and layer depth of 30-cm and 60-cm

5. Flocculent-flocs as examined by using digital image analysis

This study was done by applying the technique of digital camera visualization for analyzing flocculent-flocs. The performance of the system in terms of the floc size distribution was examined for floc number, floc size, and floc density. The investigation of floc size distributions resulting from flocculation was examined using digital camera analysis to avoid floc break apart. The digital camera recording and image analysis were used to measure the floc size and sedimentation rate. The system was under hydraulic rate of $2.5 \text{ m}^3/\text{m}^2\text{-h}$ and PACl dose of 2.5 mg/L difference media size 3-mm, 6-mm, and 10-mm. The floating-media flocculator was operated as single, dual and multilayer configuration at the layer depth of 30-cm and 60-cm.

Floc sizes distribution

Figure 41 shows floc size distributions during the whole operation time under hydraulic rate of $2.5 \text{ m}^3/\text{m}^2\text{-h}$, PACl dose of 2.5 mg/L, media size 3-mm, and layer depth of 30-cm. At 30 minutes the flocculent-floc size ranges from 56 to 168 μm , there is a peak at 56 μm , skewness

1.6680. Fine flocs size was found to be numerous, but moderate and large size were less numerous. At 6 hours the flocculent-floc size ranges from 56 to 728 μm , there is a peak at 224 μm , skewness -0.0564. Fine flocs size was found to decrease in number, but moderate and large size increased in number during operation time. The flocculent-floc size movement of the peak of the distribution toward larger size within the operation time is easily seen.

Figure 42 that shown relationship between accumulate head-loss development with number of floc during the whole operation time under hydraulic rate of $2.5 \text{ m}^3/\text{m}^2\text{-h}$, PACl dose of 2.5 mg/L, media size 3-mm, and layer depth of 30-cm. Accumulation head-loss and number of floc value continued to increase until 180 minutes. With the passage of time, as flocculent-floc accumulate within an intermedia porous space of the bead media. The head-loss through the media-layer started to build up beyond the initial value. This phenomenon was filtration. Number of floc continued to increase in number within 6 hours, but beyond 180 minutes accumulation head-loss value started stabilized. Therefore, flocculent-floc was accumulated within media-layer that flocculent-floc accumulation value within media-layer equal to flocculent-floc penetration media-layer. After some period of time, the operating head-loss reaches a determined head-loss value, and the system must be cleaned which this system did not need backwash same as filter. This phenomenon was suitable for floc formation. Overall experiments, flocculation behavior of flocs distribution and head-loss development are the same.

Figure 43-47 shows floc size distribution. Figure 43, peak at 280 μm , 280 μm , and 336 μm , maximum floc size was 728 μm , 840 μm , and 1120 μm , average floc size was 335 μm , 354 μm , and 376 μm in media sizes 3-mm, 6-mm, and 10-mm, respectively. The flocculation behavior of floating-media obtained to form floc. In this system, floc formation was link to the intermedia pore space. At a large media size, the maximum floc size occurs at about 1120 μm , at fine media size, it is seen that small flocculent-floc. The bigger-formed flocs can penetrate through the void of media. Subsequently, the collision between flocs in the intermedia pore space promoted the larger flocs (Culp, 1977; Luttinger, 1981 and Kludpiban, 2000). Thus, media bead of 10-mm (single-media) could form the largest flocculent-flocs size compared with 3-mm and 6-mm both layer depths of 30-cm and 60-cm. The intermedia pore space was 1.35 mm^2 , 3.9 mm^2 , and 6.91

mm^2 at media beads of 3-mm, 6-mm, and 10-mm in diameter, respectively. A higher layer depth (60-cm) causes a narrower size distribution of flocculent-flocs than a shorter layer depth (30-cm). From Table 5 higher layer depth found a higher velocity gradient than shorter layer depth in same media size. Because a high velocity gradient resulted in decreasing of flocculent-floc size. High velocity gradient could break up flocculent-floc size more easily than shorter layer depth. The same results were also found in Figures 43-47.

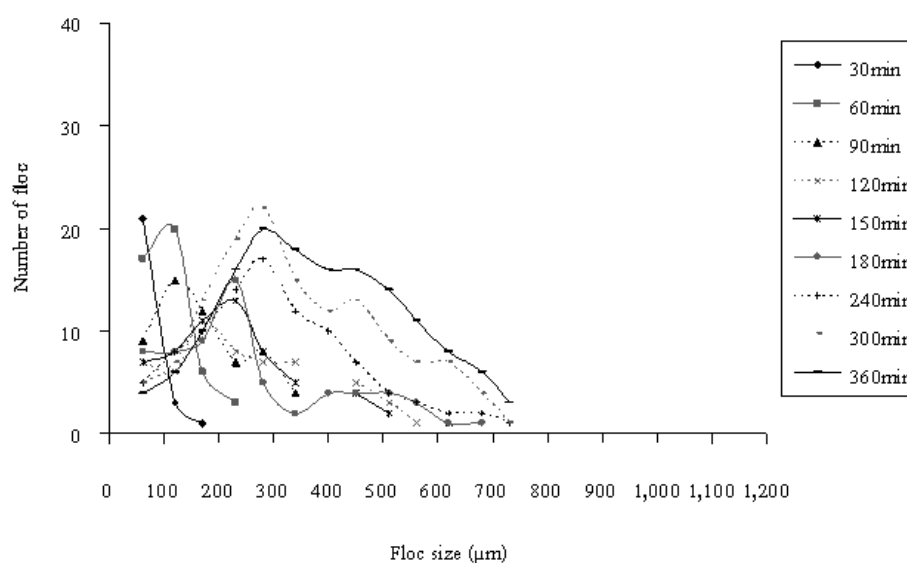


Figure 41 Floc size distribution (Media size 3-mm, layer depth 30-cm , hydraulic rate of $2.5 \text{ m}^3/\text{m}^2\text{-h}$ and PACl dose of 2.5mg/L)

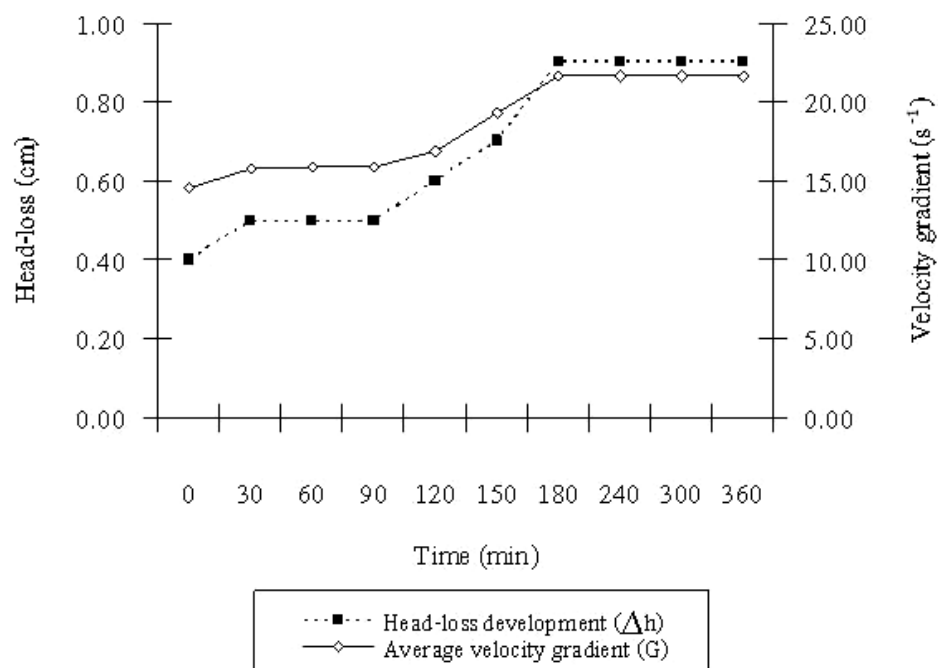


Figure 42 Head-loss development versus average velocity gradient under hydraulic rate of $2.5 \text{ m}^3/\text{m}^2\text{-h}$, PACl dose of 2.5mg/L , and 30-cm layer depth

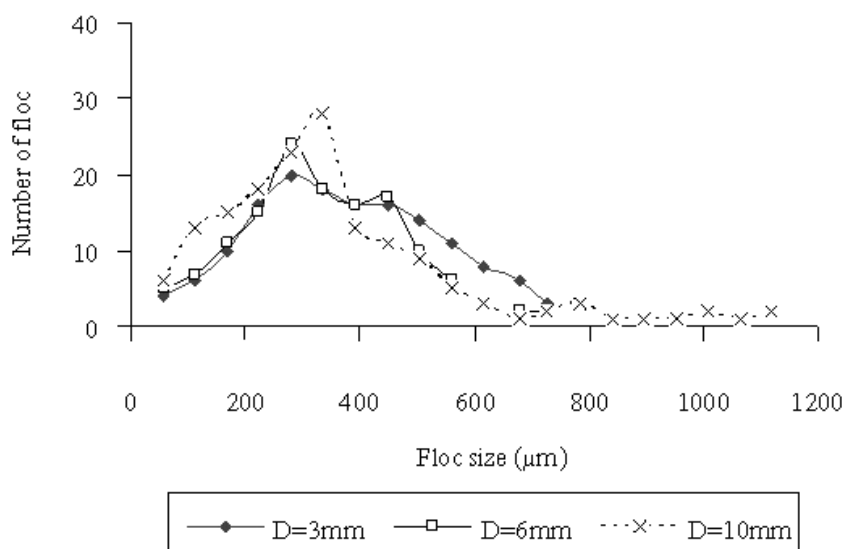


Figure 43 Floc size distribution of single-layer different media sizes (30-cm layer depth, hydraulic rate of $2.5 \text{ m}^3/\text{m}^2\text{-h}$ and PACl dose of 2.5mg/L) at 6th hour.

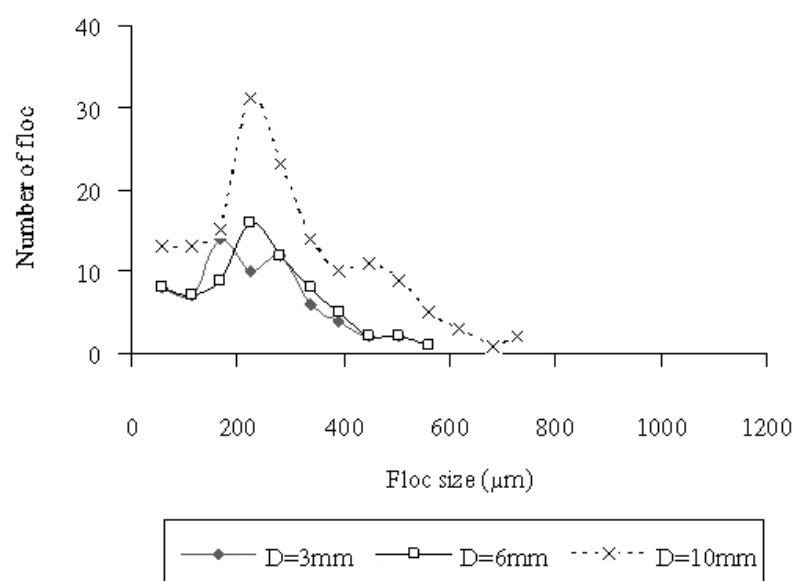


Figure 44 Floc size distribution of single-layer different media sizes (60-cm layer depth, hydraulic rate of $2.5 \text{ m}^3/\text{m}^2\text{-h}$ and PACl dose of 2.5mg/L) at 6th hour.

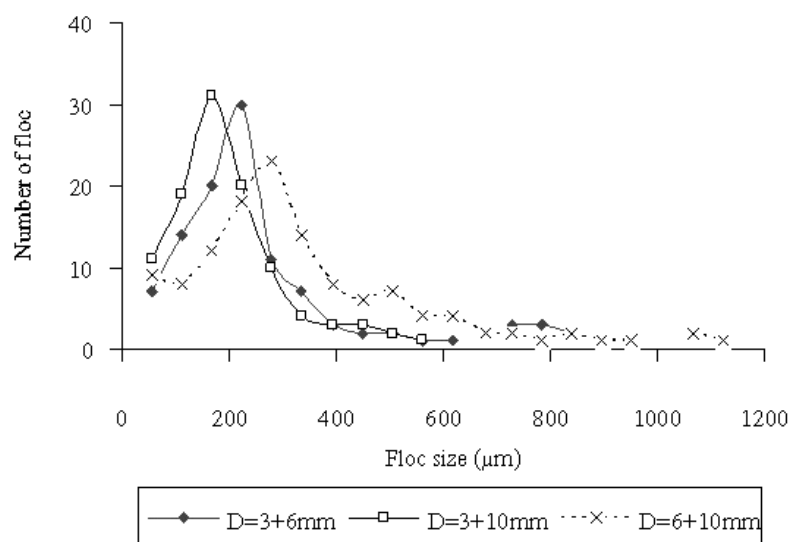


Figure 45 Floc size distribution of dual-layer different media sizes (30-cm layer depth, hydraulic rate of $2.5 \text{ m}^3/\text{m}^2\text{-h}$ and PACl dose of 2.5mg/L) at 6th hour.

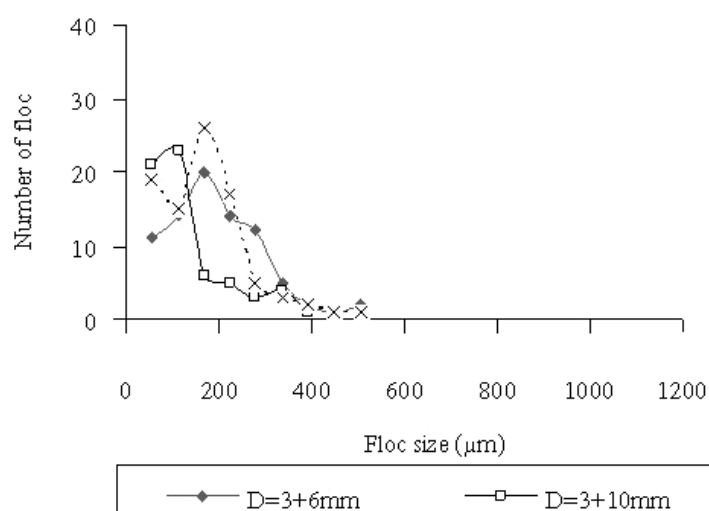


Figure 46 Floc size distribution of dual-layer different media sizes (60-cm layer depth hydraulic rate of $2.5 \text{ m}^3/\text{m}^2\text{-h}$ and PACl dose of 2.5mg/L) at 6th hour.

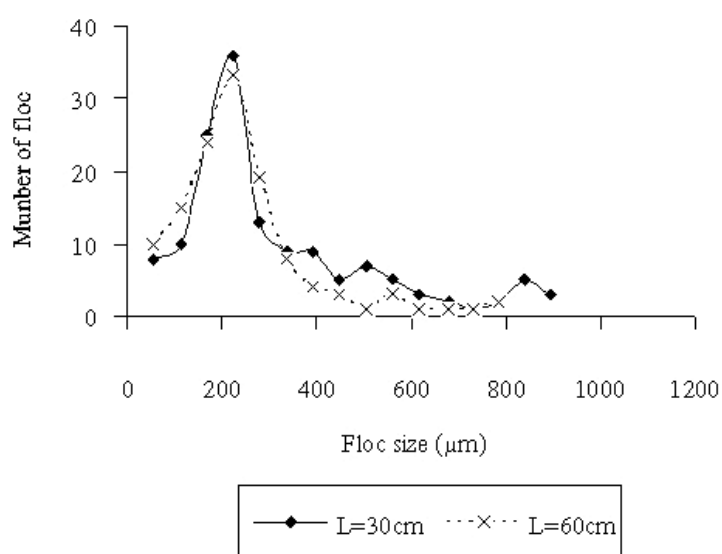


Figure 47 Floc size distribution of multilayer different media sizes, layers depth (hydraulic rate of $2.5 \text{ m}^3/\text{m}^2\text{-h}$ and PACl dose of 2.5mg/L) at 6th hour.

Floc density

The floc size and density data for flocculate-floc can provide information about the flocculent-floc interaction and its effects on the floc performance. Floc density (ρ_s) cannot be measured directly with the settling velocity occurred (w). This time period is the amount of hydraulic rate and settling velocity that was used in equation (1). The floc density was calculated by the result of equation (1) is settling velocity value to obtain in equation (2). The system was operated under the hydraulic rate of $2.5 \text{ m}^3/\text{m}^2\text{-h}$ PACl dosage of 2.5-mg/L which different of media size 3-mm, 6-mm, 10-mm in diameters and layer depth of 30 cm and 60-cm. Figure 48, during the first 120 minutes of operation time floc density value continued to increased, beyond 120 minutes floc density value decreased constantly. The same results were also found in Figures 48-52.

Table 8 shows floc density in media size of 3-mm in diameter was 1.0131 g/cm^3 and 1.0167 g/cm^3 , velocity gradient 0.9 s^{-1} and 1.1 s^{-1} , accumulate head-loss 21.7 cm and 22.4 cm, and average floc size was $336 \text{ }\mu\text{m}$ and $226 \text{ }\mu\text{m}$ at layer depth of 30-cm and 60-cm, respectively. The experimental resulted, could describe higher velocity gradient, higher accumulate head-loss and longer layer depth that produced dense compactness of floc, but small floc size.

Figure 53 shows the value of floc density versus maximum floc size. The small floc size results in better settling floc than big floc size. Effective floc density significantly changed with flocculent-floc size. Flocs are typically fractal objects, whose density decreases with increasing floc size (Gregory, 1998).

Table 8 Performance of floating media system

Run no.	Media size (mm)			layer depth (cm)	Velocity gradient (s^{-1}); G	Accumulate head-loss (cm); Δh_L	Average floc size (μm); d_s	Average floc density (g/cm^3); ρ_s
14	3	-	-	30	21.7	0.9	336	1.0131
15	3	-	-	60	22.4	1.1	226	1.0167
16	6	-	-	30	13.3	0.3	354	1.0289
17	6	-	-	60	14	0.4	240	1.0370
18	10	-	-	30	11	0.2	376	1.0247
19	10	-	-	60	11.5	0.4	286	1.0442
20	3	6	-	30	16.6	0.4	264	1.0292
21	3	6	-	60	17.3	0.8	197	1.0756
22	3	10	-	60	16.9	0.6	199	1.0536
23	3	10	-	60	17.7	0.9	134	1.0694
24	6	10	-	30	13.3	0.25	344	1.0258
25	6	10	-	60	13.6	0.5	209	1.0502
26	3	6	10	30	15.8	0.4	315	1.0399
27	3	6	10	60	16	0.7	243	1.0674

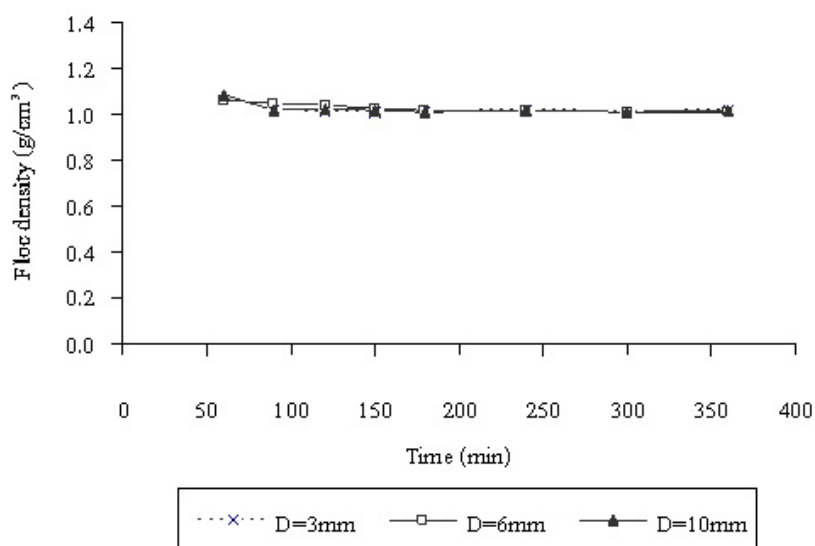


Figure 48 Floc density of single-layer different media size 3-mm, 6-mm and 10-mm bead diameter (30-cm layer depth, hydraulic rate of $2.5 m^3/m^2 \cdot h$ and PACl dose of $2.5 mg/L$)

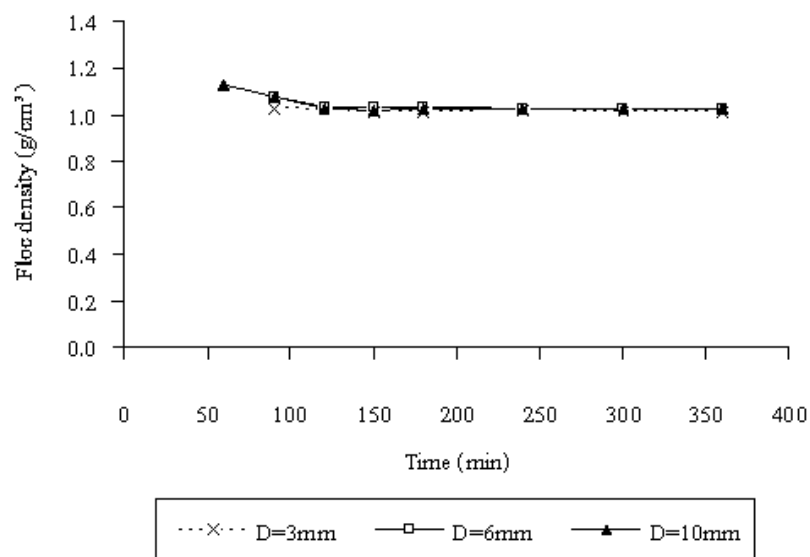


Figure 49 Floc density of single-layer different media size 3-mm, 6-mm and 10-mm bead diameter (60-cm layer depth, hydraulic rate of $2.5 \text{ m}^3/\text{m}^2\text{-h}$ and PACl dose of 2.5mg/L)

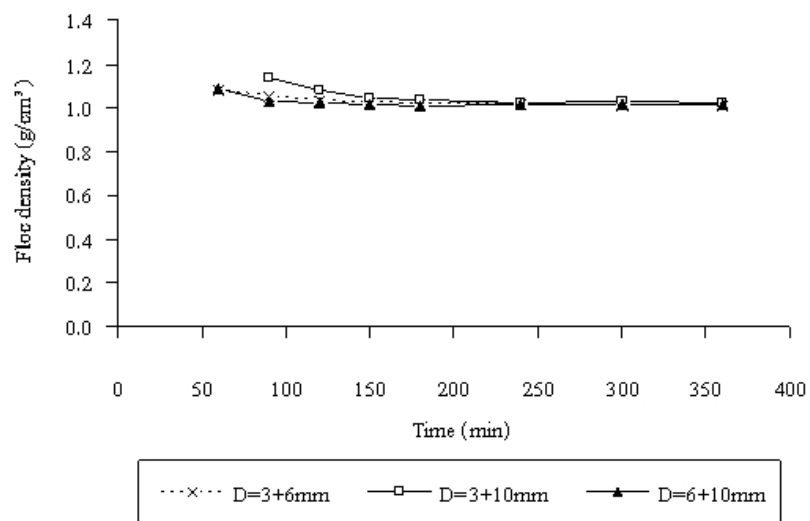


Figure 50 Floc density of dual-layer different media size 3-mm, 6-mm and 10-mm bead diameter (30-cm layer depth, hydraulic rate of $2.5 \text{ m}^3/\text{m}^2\text{-h}$ and PACl dose of 2.5mg/L)

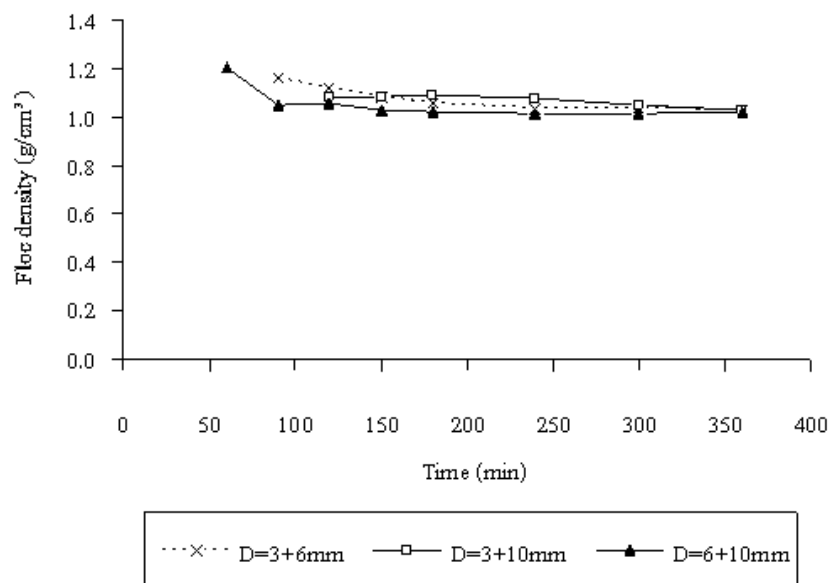


Figure 51 Floc density of dual-layer different media size 3-mm, 6-mm and 10-mm bead diameter (60-cm layer depth, hydraulic rate of $2.5 \text{ m}^3/\text{m}^2\text{-h}$ and PACl dose of 2.5mg/L)

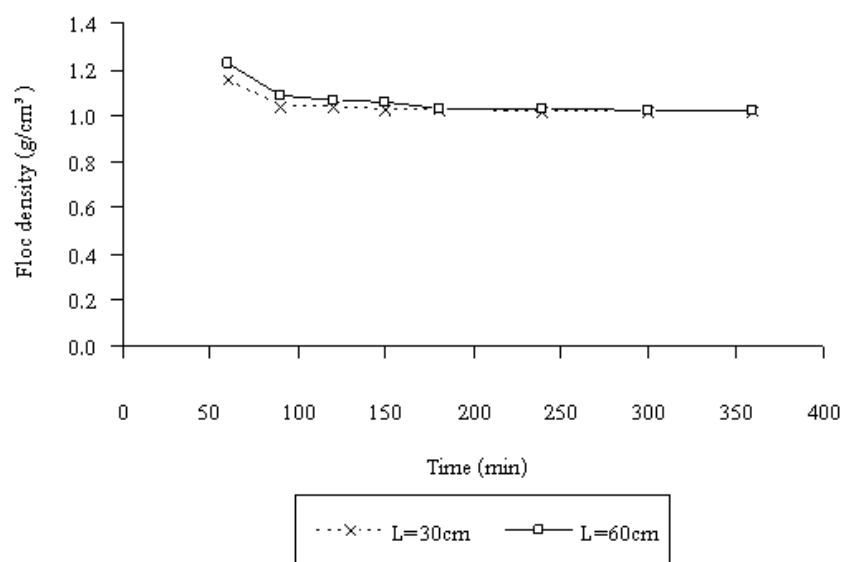


Figure 52 Floc density of multilayer different media size 3-mm, 6-mm and 10-mm bead diameter, 30-cm and 60-cm layer depth (hydraulic rate of $2.5 \text{ m}^3/\text{m}^2\text{-h}$ and PACl dose of 2.5mg/L)

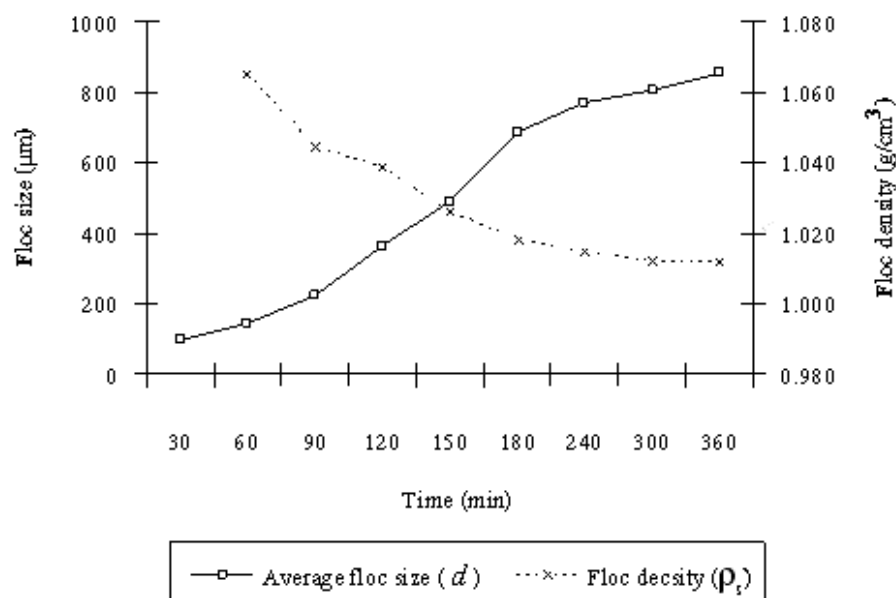


Figure 53 Floc density versus average floc size flocculator under hydraulic rate of $2.5 \text{ m}^3/\text{m}^2\text{-h}$, PACl dose of 2.5 mg/L , and 30-cm layer depth

6. Flocculent-flocs size was compared by using both techniques

This study was done by applying the technique of digital camera visualization for analyzing flocculent-flocs to compare the results with the conventional technique of microscopic analysis. The investigation of flocculent floc size resulted from flocculation were examined using a digital camera analysis to avoid of floc breakage. The system was under hydraulic rate of $2.5 \text{ m}^3/\text{m}^2\text{-h}$ and PACl dose of 2.5 mg/L .

From Figure 54, the comparison between the floc size measure by a microscopic analysis (d_M) and floc size analyzed by digital image analysis (d_D) was carried out can be seen. The average floc size of digital image continued to increase in size from 82 μm to 692 μm within 6 hours, but the maximum floc size (95 μm) of microscopic analysis decreased until 120 minutes and stabilized at maximum floc size at 120 minutes (65 μm).

The effective flocculent-floc size did not differ significantly between conventional analysis and image analysis. Because microscopy requires samples to be withdrawn and the

particle to be pass through a small orifice, which may cause the floc to break apart and disperse (Gibbs, 1982). Floc could break-up easily during sampling and handling in two ways of floc rupture. These have been classified as surface erosion and large-scale fragmentation. Small-scale is surface erosion, erosion is due to the shear force act with floc surface resulting in an increase in the small floc size ranges. Large-scale is fragmentation that is thought to occur from tensile stress acting normally across the whole floc (Jarvisa et al., 2005). Microscopy could not perform realistic floc size without disruption and breaking during sample collection and measuring.

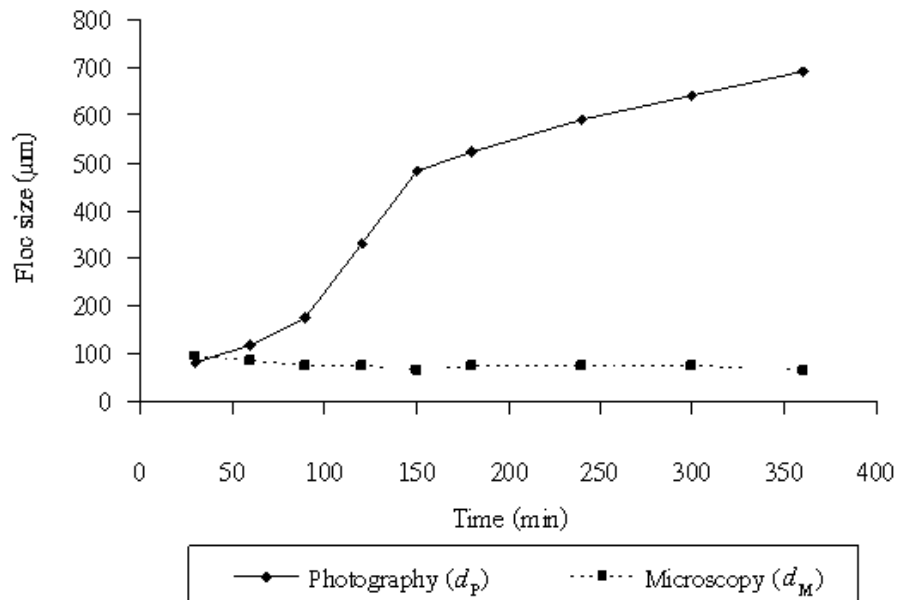


Figure 54 Relationship between of the average floc size of microscopic analysis (d_M) and the average floc size of digital image analysis (d_p) (3-mm bead diameter, 30-cm layer depth, hydraulic rate of $2.5 \text{ m}^3/\text{m}^2\text{-h}$ and PACl dose of 2.5 mg/L)

CONCLUSION

1. Image analysis was an optical floc sampling technique which did not intrude the system and did not destroy flocculent-floc. This technique could be used to measure number, size, and density of flocculent-floc. Resolution image consisted of 2120 (horizontal) x 2816 (vertical) pixels. Each pixel records using 24-bits, there are 256 gray scale levels for each image pixel in size. The camera lens was macro lens with ISO 200, bracketing $\pm 1/3$ EV, F-6.3, shutter exposure of 1/800 sec and flash ± 0 were found to provide good results for images. A digital camera was set in front of the column which was illuminated by 3 light-sources on the opposite side of the column to provide back-lighting. The floc images were viewed as shadows. Flocculent-floc below 56 μm could not be reliably measured using this camera system. Video pictures were low resolution (320 x 245 pixels) so flocculent-floc sizes below 150 μm could not be measured. The flocculent-flocs were compared with microscopic analysis and image analysis. The flocculent-floc sizes did not correspond between microscopic technique and photographic technique. This was because microscopic analysis could not measure realistic floc size without floc disruption and breaking during sampling and handling. Photography as a technique for the quantification of particle size and shape is more accurate than microscopy. During the first 3 hours, phenomenon in the system were the same as filtration, but after the first 3 hours phenomenon in the system was flocculation. Because accumulation head-loss value started stabilizing at 180 minutes, the system did not need backwashing and flocculent-floc continued to increase in size the whole operating time. At the initial period of time floc size distributions, fine flocs size was found to be numerous, but moderate and large size were less numerous. With the passage of time, fine flocs size was found to decrease in number, but moderate and large size increased in number during operation time. The flocculent-floc size could observe movement of the peak of the distribution toward larger size. Floc density in comparison to flocculent-floc size significantly changed in that density decreases with increasing floc size. High floc density required high velocity gradient, high accumulate head-loss, and high detention time, but produced small floc size.

2. The floating media flocculator required low flocculent dosage to yield the large floc size and the low head-loss development. The higher dosage caused the higher head loss

development. The high dose led to greater clogging, the flocculation mechanisms in the floating-media column, larger expansion of floating media depth and quicker detachment of flocs from media. The low hydraulic rate produced the large floc size and the low head-loss development. Increasing the hydraulic rate increased the floc rate deposit on the floating beads. This had an additional effect of increasing the intermedia shear forces. If the shear forces exceeded the attachment forces, floc could push from the surface of media prior to capture. The high hydraulic rates provided higher head loss development for all PACl doses because the head loss caused floc volume to be retained in the media bed. The high hydraulic rate decreased the floc formation to promote flocculent-floc. The velocity gradient was dictated by head-loss. The head-loss was a function of hydraulic rate. Shear forces due to too high velocity gradient could break up larger floc and limit the flocculent-floc size. The optimum hydraulic rate and PACl dose were $2.5 \text{ m}^3/\text{m}^2\text{-h}$ and 2.5 mg/L , the highest turbidity removal of 95.2%, the maximum floc size of digital image analysis of $327 \text{ }\mu\text{m}$, maximum floc size of microscopic analysis of $60 \text{ }\mu\text{m}$, floc density 1.0343 g/cm^3 , and the lowest head-loss development of 10 mm were achieved in this optimum condition. The multilayer floating media had several advantages over the single media in order to perform the better system performances such as low head-loss development and large floc formation. The increasing media size resulted in the decrease of head loss development and the increasing of average floc size.

RECOMMENDATION

1. The column should be flat observation region for high resolution images and sufficient to analyze.
2. The system should be operated in long term for obtaining the steady-state floc size.

LITERATURE CITED

- Adin, A. and Rebhun, M. High-rate contact flocculation-filtration with cationonic polyelectrolytes. **J.AWWA**. 1974, 66: 109-117.
- Ben Aim, R., Shanoun, A., Visvanathan, C., and Vigneswaran, S. 1993. New filtration media and their sue in water treatment. **Proc. World filter congress**, Nagoya, Japan, pp. 273-276.
- Blazier, A.A. 2003. Experimental Evaluation of temporal Particle Agglomeration and Metal Partitioning of urban Rainfall Runoff. M.S. thesis, Louisiana State University.
- Cheermisinoff, N.P. 1995. **Handbook of water and Waster Treatment Technology**. Marcel Dekker, Inc., New York.
- Chiemchaisri, C., Panchawaranon, C., Rutchatanunt, S., Kludpiban, A., Ngo, H.H. and Vigneswaran, S. 2003. Development of floating plastic media filtration system for water treatment and wastewater reuse. **Environ Sci Health A Tox Hazard Subst Environ Eng**. 38 (10):2359-2368.
- Culp, R.L., 1977. Direct filtration. **J. AWWA**. 69: 375-378.
- Eisma, D. 1986. Flocculation and deflocculation of suspended matter in estuaries. *Neth. J. sea Res.* 20, 183-99.
- Gibbs, R.J., Floc Breakage during HIAC Light-Blocking Analysis., **Environmental science and technology**. 1982, 16, 298-299.
- Graham, T. On the Properties of Silicic Acid and Other Analogous Colloidal Substances, **Journal of the Chemical Society of London**, 1864, 17, 318-323

Gregory, H. Fundamentals of flocculation. **CRC Crit Rev Environ Control**. 1989. 19(3):185-230.

Innerfeld, H., Forndran, A., Ruggiero, D.D., and Hartman, J.J. 1979. Dual process high-rate filtration of raw sanitary sewage and combined sewer overflows. EPA-600/2-L79-015 (PB296626/AS).

Jarvis, P., Jefferson, B., Gregory, J. and Parsons, S.A. 2005. A review of floc strength and breakage. **Water Res.** 39: 3121–3137.

Kawamura, S. 1991. Integrated Design and Operation of Water Treatment Facilities. 2nd ed. John Wiley and Sons Inc., New York.

Kludipiban, A. 2000. **Turbidity Removal in Downflow Filtration System Using Floating Plastic Media Bed in Water Treatment**. M.S. thesis, Kasetsart University.

Lee, D.J., Chen, G.W., Liao, Y.C., Hsieh, C.C., **Water Res.** 30 .1996. 541.

Luttinger, L.B. 1981. The use of polyelectrolyte in filtration process. In L.K. William Schwoyer (ed.). **Polyelectrolytes for Water and Wastewater Treatment**. Boca Raton., Florida.

Metcalf and Eddy. 2003. **Wastewater Engineering Treatment and Reuse**. 4th ed. McGraw-Hill Companies, Inc., New York.

Ngo, H.H., Vigneswaran, S., 1995b. Application of downflow floating medium flocculator/ prefilter (DFF)-coarse sand filter (CSF) in nutrient removal. 3rd Intl. Conf.

O'Melia, C.R., and Ali, W. 1978. The role of retained particles in deep bed filtration. **Prog. Wat. Tech.** 10 (5/6): 167-182.

Peter Kroll, Constanze La Dous, Hans-Jürgen Bräuer ,Verlag Herri Deutsch, Frankfurt am Main (1999),: **"Treasure Hunting in Astronomical Plate Archives"** (Proceedings of the international Workshop held at Sonneberg Observatory, March 4 to 6, 1999.)

Ravina, L. and Moramarco, N. 1993. Everything You Want to Know about Coagulation& Flocculation. **'Zeta-Meter,Inc. Available Source'**: November 5, 2004.

Reynolds, T.D., Richards, P.A. 1996. **Unit Operation and Processes in Environmental Engineering. 2nd ed.** PWS publishing Company., Boston.

Schulz, Christopher, R., Singer, P.C., Gandley, R. and Nix, J.E. 1994. Eavaluating buoyant coarse media flocculation. **JAWWA**, 86(8), 51-62.

Tipler, Paul (2004). Physics for Scientists and Engineers: **Electricity, Magnetism, Light, and Elementary Modern Physics (5th ed.)**, W. H. Freeman.

Tyson, R V. 1990. Automated transmitted light kerogen typing by image analysis: 1. **General aspects and program description**: Mededelingen Rijks Geologische Dienst, v. 45, p 139-49.

Weiner, B.B. **A Guide to Choosing a Particle Sizer from Brookhaven Instruments Corporation**. Available Source: <http://www.particlesize.com/howto.htm>, October 16, 2005.